

TCS AI-based Alloy Database (TCAL)

Validation and Calculation Examples Collection



Contents

About the Database Examples	4
TCS Al-based Alloy Database (TCAL) Resources	5
TCAL Validation Examples	7
Solidification: Phase Formation	8
Solidification: Hot Tearing Susceptibility	10
Solidification: Back Diffusion	14
Solidification: Microsegregation	15
Homogenization / Solution Treatments: Al-Si Alloys	17
Homogenization / Solution / Aging Treatments: PA Alloy	18
Homogenization / Solution / Aging Treatment: 6005	22
Electrical Resistivity and Thermal Conductivity	25
Surface Tension of Two Alloys: A356 and Alufont-47	28
Viscosity of Various Alloys	31
TCAL Calculation Examples	33
Al-Li	34
Al-Er	36
Al-Fe-Si	37
Al-Mn-Si	39
Al-Fe-Mn-Si	40
Al-Cu-Mg-Zn	41
Al-Cu-Mg-Si	43
Minor Alloying Elements	44
Al-Ce-Mg	46
Molar Volume and Related Examples	47
Metastable Phases / Precipitates	50

Electrical Resistivity and Thermal Conductivity	52
Viscosity: Al-Cu and Cu-Al-Si	57
Surface Tension: Al-Cu and Ag-Al-Cu	59

About the Database Examples

The *Validation and Calculation Examples Collection* that is available for many databases demonstrates both the *validity* of the database itself as well as demonstrates some of its *calculation* capabilities when combined with Thermo-Calc software and its Add-on Modules and features.



For each database, the type and number of available examples varies. In some cases an example can belong to both a validation and calculation type.

- *Validation* examples generally include experimental data in the plot or diagram to show how close to the predicted data sets the Thermo-Calc calculations are. It uses the most recent version of the software and relevant database(s) unless otherwise specified.
- *Calculation* examples are intended to demonstrate a use case of the database. This might be showing a binary or ternary system calculated in a phase diagram, or demonstrate how the database and relevant software features would be applied to a heat treatment application, process metallurgy, soldering process, and so forth. In the case of heat treatment, it might include the result of calculating solidification segregation, determining homogenization temperature and then predicting the time needed to homogenize. There are many other examples specifically related to each database.



Where relevant, most references related to each example set are included at the end of the individual section. You can also find additional references specific to the database itself when using the database within Thermo-Calc. You can also contact us directly should you have any questions.



If you are interested in sharing your own examples using Thermo-Calc products in unique or surprising ways, or if you want to share your results from a peer reviewed paper, send an email to info@thermocalc.com.

TCS Al-based Alloy Database (TCAL) Resources

Information about the database is available on our website and in the Thermo-Calc software online Help.

- **Website:** On our website the information is both searchable and the database specific PDFs are available to download.
- **Online Help:** Technical database information is included with the Thermo-Calc software online Help. When in Thermo-Calc, press F1 to search for the same information as is contained in the PDF documents described. Depending on the database, there are additional examples available on the website.

Database Specific Documentation

- The *TCS Al-based Alloy Database (TCAL) Technical Information* PDF document contains version specific information such as the binary, ternary, and higher-order assessed systems, phases, and models. It also includes details about the properties data (e.g. viscosity, surface tension, etc.), a list of the included elements, and summaries of the database revision history by version.
- The *TCS Al-based Alloy Database (TCAL) Validation and Calculation Examples Collection* PDF document contains a series of validation examples using experimental data, and a set of calculation examples showing some of the ways the database can be used.



Go to the [Aluminum-based Alloys Databases](#) page on our website where you can access a Validation and Calculation Examples Collection and the Technical Information plus learn more about the compatible kinetic database. Also explore further [applications of Thermo-Calc to aluminum](#) including links to resources such as publications, webinars, videos, and more.

The CALPHAD Method

The Thermo-Calc databases are developed with the CALPHAD approach based on various types of experimental data and theoretical values (e.g. those from first-principles calculations). It is based on the critical evaluation of binary, ternary, and for some databases, important higher order systems. This enables predictions to be made for multicomponent systems and alloys of industrial importance. Among these, the thermodynamic database is of fundamental importance.



For more learning resources about CALPHAD and our databases, visit the video tutorials on our [website](#) or our [YouTube playlist](#).



Learn more on our website about the [CALPHAD Method](#) and how it is applied to the Thermo-Calc databases.

TCAL Validation Examples



Some diagrams are calculated with earlier versions of the database. Negligible differences might be observed if these are recalculated with the most recent version. The diagrams are updated when there are considerable or significant improvements.

In this section:

Solidification: Phase Formation	8
Solidification: Hot Tearing Susceptibility	10
Solidification: Back Diffusion	14
Solidification: Microsegregation	15
Homogenization / Solution Treatments: Al-Si Alloys	17
Homogenization / Solution / Aging Treatments: PA Alloy	18
Homogenization / Solution /Aging Treatment: 6005	22
Electrical Resistivity and Thermal Conductivity	25
Surface Tension of Two Alloys: A356 and Alufont-47	28
Viscosity of Various Alloys	31

Solidification: Phase Formation

A conventional Scheil simulation provides an upper boundary for how far a solidification can deviate from equilibrium, therefore a real solidification is expected to occur between the equilibrium simulation and the Scheil simulation. In Thermo-Calc performing a Scheil simulation always triggers an equilibrium simulation.



Read more about [Scheil Solidification Simulations](#) on our website, including [how to select the right model for your simulation](#). If you are in Thermo-Calc, press F1 to search the help to learn about using Scheil.

A206 Alloy

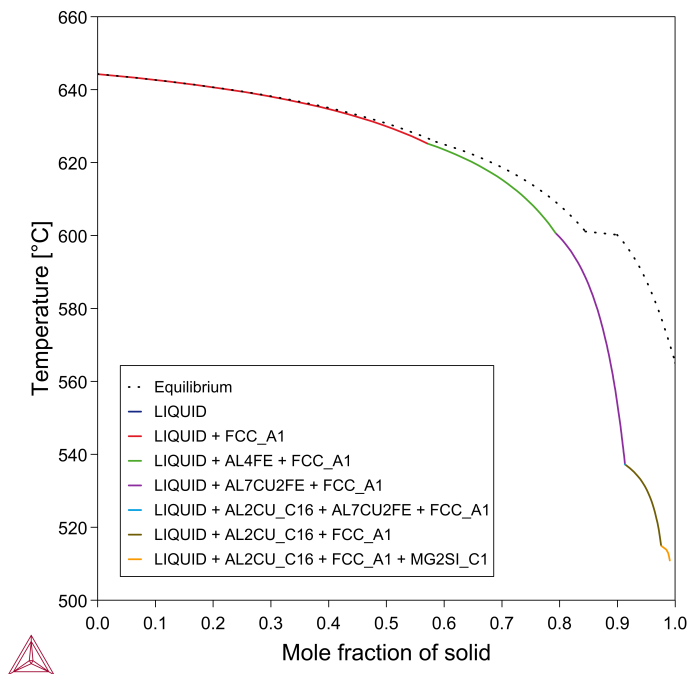


Figure 1: Scheil solidification of an A206 alloy (Al-4.58Cu-0.28Mg-0.51Fe-0.07Si-0.003Mn, wt.%) with the $Al_{13}Fe_4$ and Al_6Mn phases suspended. According Liu et al. [2012Liu], the metastable Al_mFe (modeled as Al_4Fe) Fe phase formed after (Al) during the solidification. The phase formation sequence and phase transformation temperatures can be well accounted for with this calculation.

Alloy AA7075

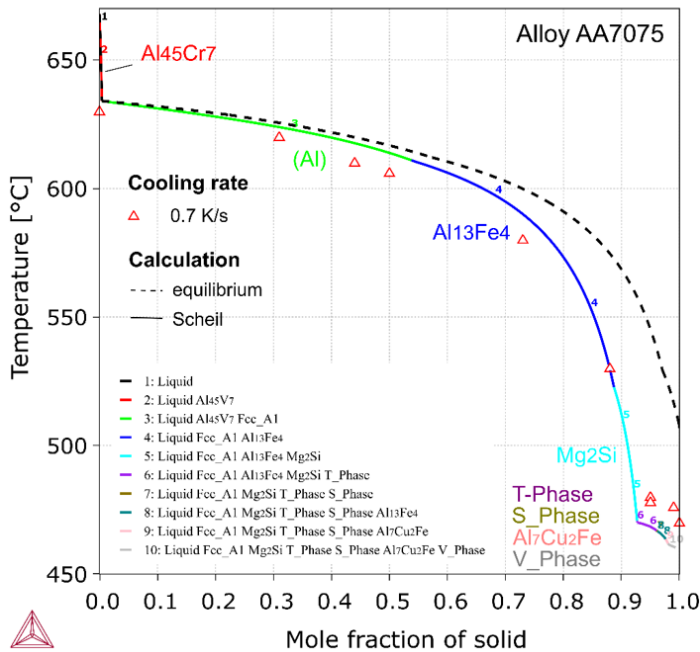


Figure 2: Equilibrium solidification and Scheil solidification simulations of alloy AA7075, compared with experimental results [1990Bac]. (Al), $Al_{13}Fe_4$, Mg_2Si , T-Phase and V-Phase ($MgZn_2$) are found in the microstructure as predicted from the calculation. $Al_{45}Cr_7$ forms primarily as a Cr-bearing phase, which may have been overlooked in experimental investigation due to its small amount. S-Phase was shown at the late stage of the Scheil solidification and its amount is small. Al_2Cu was experimentally observed but not shown in the calculation.

References

- [1990Bac] L. Backerud, G. Chai, J. Tamminen, Solidification Characteristics of Aluminum Alloys in Foundry Alloys, Volume 1 and 2 (American Foundrymen's Society, Inc., 1990), p. 266.
- [2012Liu] K. Liu, X. Cao, X. G. Chen, A New Iron-Rich Intermetallic-Al m Fe Phase in Al-4.6Cu-0.5Fe Cast Alloy. Metall. Mater. Trans. A. 43, 1097–1101 (2012).

Solidification: Hot Tearing Susceptibility

It is found that hot tearing susceptibility of aluminum alloys can be reasonably predicted via evaluating the terminal freezing range (TFR). In general, the wider the TFR is, the more the alloy is susceptible to hot tearing.

AA7075

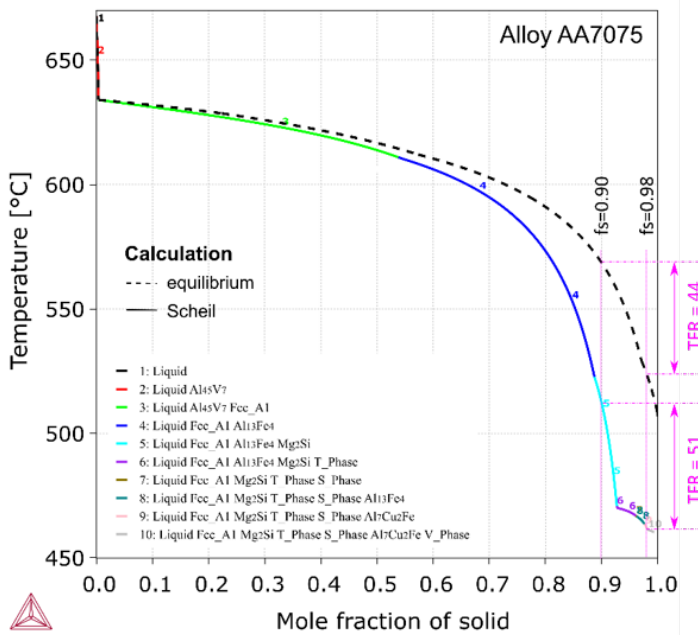


Figure 3: AA7075 alloy has a large TFR (44-51) and is prone to hot tearing.

A356.1

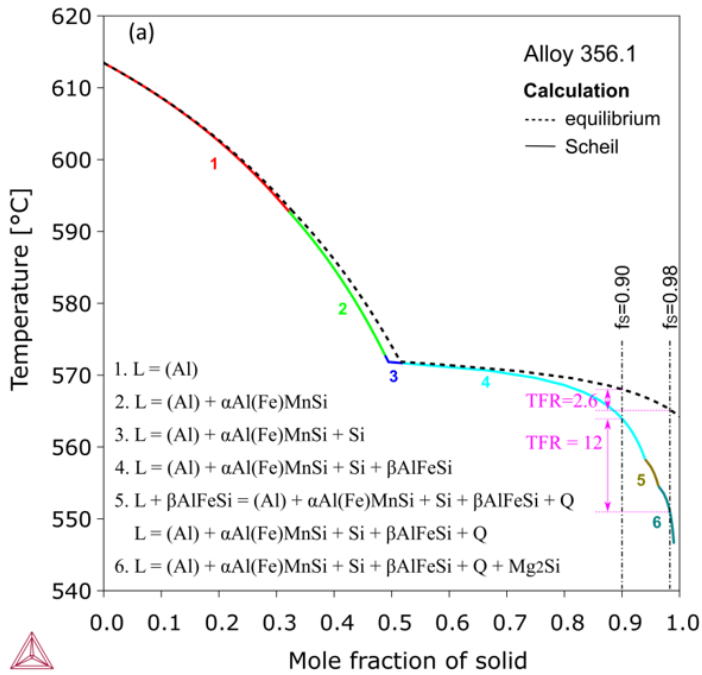


Figure 4: A356.1 alloy has a much lower TFR (2.6-12) and is much less susceptible to hot tearing. Equilibrium calculation shows an even lower value of TFR (2.6) than the Scheil simulation. This may indicate that the risk of hot tearing may be reduced by changing experimental conditions, e.g. lowering the cooling rate or using preheated casting molds.

AA3000

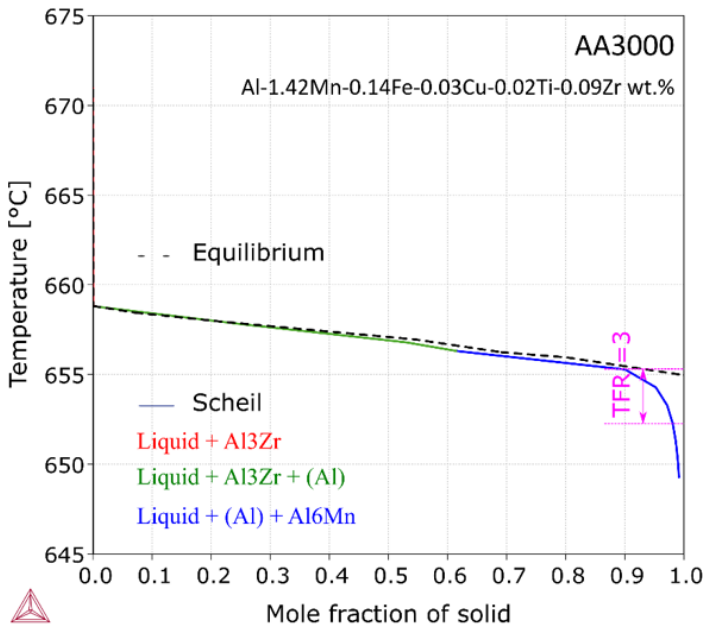


Figure 5: AA3000 alloy has an even lower TFR and has been reported to be unsusceptible to hot tearing.

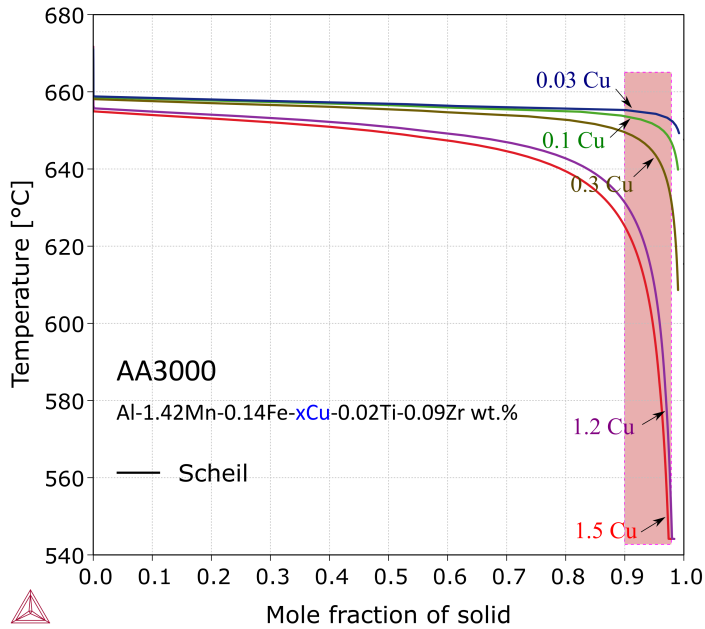


Figure 6: Adding Cu to AA3000 alloy significantly increases the susceptibility and worsens the castability.

3000 Series Alloys with Cu Additions

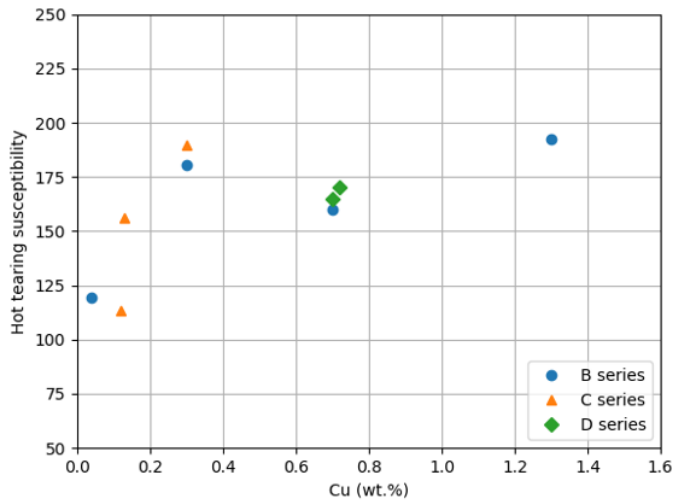


Figure 7: The recent experimental investigations by Razaz [2019Raz] reported that "a similar increase in HTS with Cu additions from 0.3 to 1.2 wt.% was proven" in 3000 alloys. The data are somewhat scattered because there are three groups of alloys and the contents of the other alloying elements are not exactly the same even for each group, but one can evidently see the trend that HTS increases with Cu additions.

Reference

[2019Raz] G. Razaz, T. Carlberg, Hot Tearing Susceptibility of AA3000 Aluminum Alloy Containing Cu, Ti, and Zr, *Metall. Mater. Trans. A Phys. Metall. Mater. Sci.*, (2019).

Solidification: Back Diffusion

An experimental solidification is usually expected to be between the equilibrium calculation and the classic Scheil simulation. The deviation from a Scheil simulation may be due to the effect of back diffusion. To better predict or account for the phase formation during the experiment, you can run a Scheil simulation considering back diffusion.

The example shows three solidification simulations of the A204.2 foundry alloy. One is run without back diffusion and labeled *Classic Scheil*. The one with back diffusion is run at a cooling rate of 0.2 K/s. The dashed line shows the results from an equilibrium simulation.

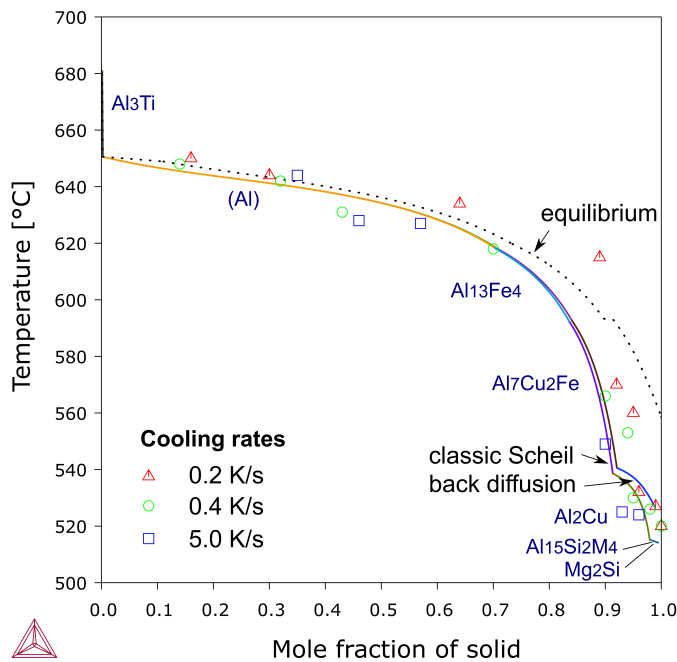


Figure 8: Solidification simulations of foundry alloy 204.2 ($\text{Al-Si}_{0.08}\text{Fe}_{0.20}\text{Cu}_{4.40}\text{Mn}_{0.02}\text{Mg}_{0.22}\text{Ti}_{0.22}$, wt.%), compared with DTA experimental results [1990Bac]. The formation of (Al), $\text{Al}_{13}\text{Fe}_4$, $\text{Al}_7\text{Cu}_2\text{Fe}$ and Al_2Cu was reproduced in the Scheil simulation. Al_3Ti appeared as the primary phase due to the Ti addition.

Reference

[1990Bac] L. Backerud, G. Chai, J. Tamminen, Solidification Characteristics of Aluminum Alloys in Foundry Alloys, Volume 1 and 2 (American Foundrymen's Society, Inc., 1990), p. 266.

Solidification: Microsegregation

Microsegregation can be easily predicted by the formation of grain boundaries phases and the composition profile of the (Al) matrix phase. The former has been demonstrated in another example, [Solidification: Phase Formation](#). [Figure 9](#) shows the (Al) profiles in Al-2, 4, and 8 wt.% Cu alloys from Scheil simulations using the TCS Al-based Alloy Database (TCAL). In the [Figure 10](#) micrograph, the simulated profiles indicate that:

- The cores of (Al) grains are lean in Cu. Increasing the alloy composition increases the Cu content in the cores.
- The maximum Cu content in the outer rims of (Al) grains is independent of the alloy composition.
- The outer rims are thickened with increasing the Cu content in the alloys.

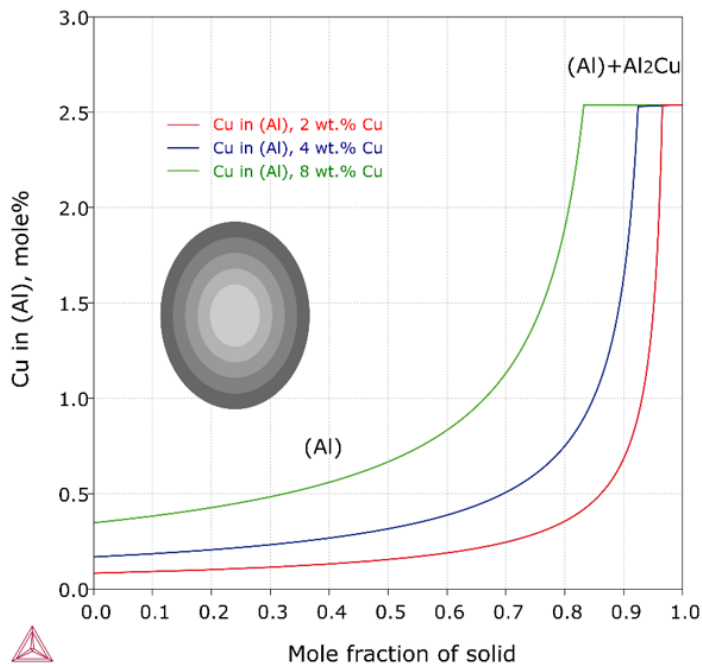


Figure 9: The (Al) profiles in Al-2, 4, and 8 wt.% Cu alloys from Scheil simulations.

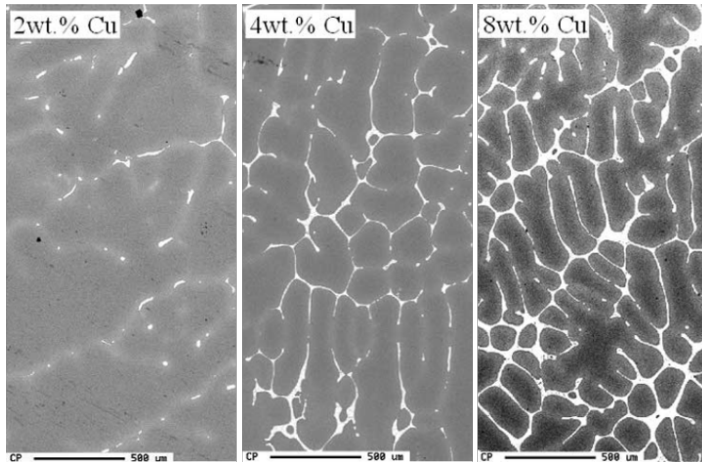


Figure 10: A micrograph from Kurum [2005Kur]. Details described in the text.

Reference

[2005Kur] E. C. Kurum, H. B. Dong, J. D. Hunt, Microsegregation in Al-Cu Alloys. *Metall. Mater. Trans. A*, 36, 3103 (2005).

Homogenization / Solution Treatments: Al-Si Alloys

In some cases, the heating temperature can only be preliminarily determined with a stepping calculation. It should be optimized, together with the heating time, based on the Diffusion Module (DICTRA) simulations.

This example, using the TCS Al-based Alloy Database (TCAL), shows simulated dissolution of Si particles at 500 °C, 530 °C, and 560 °C with a multiple-cell approach (Figure 11). 500 °C is too low since the particles cannot be fully dissolved even after three (3) hours. By comparison, the particles disappear within 15 minutes at 560 °C and one (1) hour at 530 °C. You can choose either temperature or a temperature between taking into account other factors, such as energy consumptions, risks of melting, etc.



Read more about the [Diffusion Module \(DICTRA\)](#) on our website. There is also a [Getting Started with the Diffusion Module \(DICTRA\)](#) page available. If you are in Thermo-Calc, press F1 to search the help to learn about the available settings included with the Add-on Module.

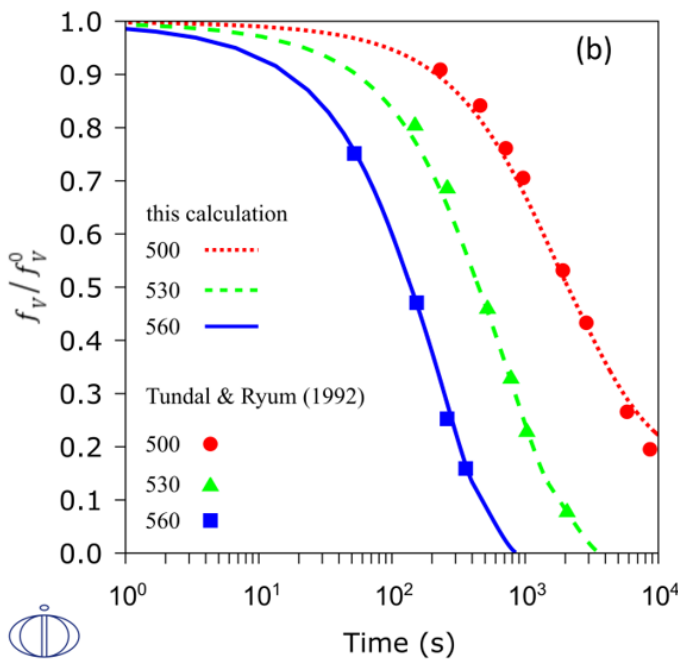


Figure 11: Simulated dissolution of Si particles at 500 °C, 530 °C, and 560 °C for multiple-cell approaches.

Homogenization / Solution / Aging Treatments: PA Alloy

Solution treatment is to dissolve (fully or partly) particles that form at the grain boundaries into the (Al) matrix. *Homogenization* is to eliminate or reduce the composition segregation in the (Al) matrix. Very often these kinds of treatments can be performed at the same time and thus are not distinguished. Temperature and time are the most important parameters that need to be optimized for a heat treatment.

For a solution treatment, the heating temperature can be preliminarily determined according to an equilibrium stepping shown below. A narrow window of 462-475 °C of single (Al) phase was predicted for alloy PA Alloy: Al-10.3Zn-1.6Cu-2Mg, wt. %. In such cases, the temperature may be determined as the mean value independently of the heating time. This agrees well with the experimental temperature of 470 °C by Marlaud [2010Mar].

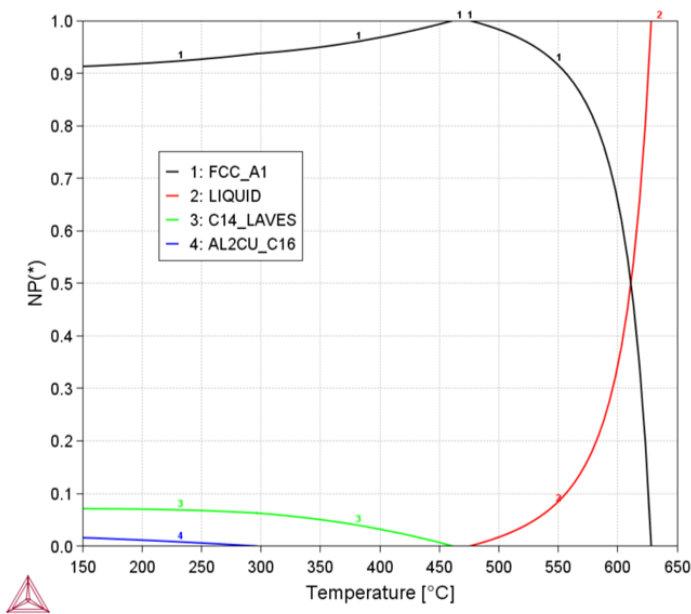


Figure 12: Solution treatment showing a narrow window of 462-475 °C of single (Al) phase which was predicted for the PA Alloy (Al-10.3Zn-1.6Cu-2Mg, wt. %).

Uncertainty Calculation with the Property Model Calculator

The alloy may deviate from its nominal composition. It is useful to investigate how the composition uncertainty affects the temperature window of the single-(Al)-phase region. With the Property Model Calculator in Thermo-Calc Graphical Mode you can easily take into account such uncertainties in calculations. A three percent (3 %) tolerance level was assumed for the contents of the major alloying elements, i.e. Zn 10.3 ± 0.3 , Cu 1.6 ± 0.05 and Mg 2.0 ± 0.06 , wt.%.

A sample of 200 compositions is done within the ranges according to a Gaussian distribution and calculated transition temperatures for C14_Laves / FCC_A1 and FCC_A1 / Liquid. [Figure 13](#) plots the frequency of each obtained temperature. A single (Al) phase can be attained for all the sampled compositions, while the window is further narrowed down. The heating temperature of 470 °C is good in most cases but a bit too high at several compositions.



Read more on our website about [Property Models](#), including information about the material specific Model Libraries (i.e steel, nickel, titanium, etc.), as well as how to create your own custom models in TC-Python. If you are in Thermo-Calc, press F1 to search the help.

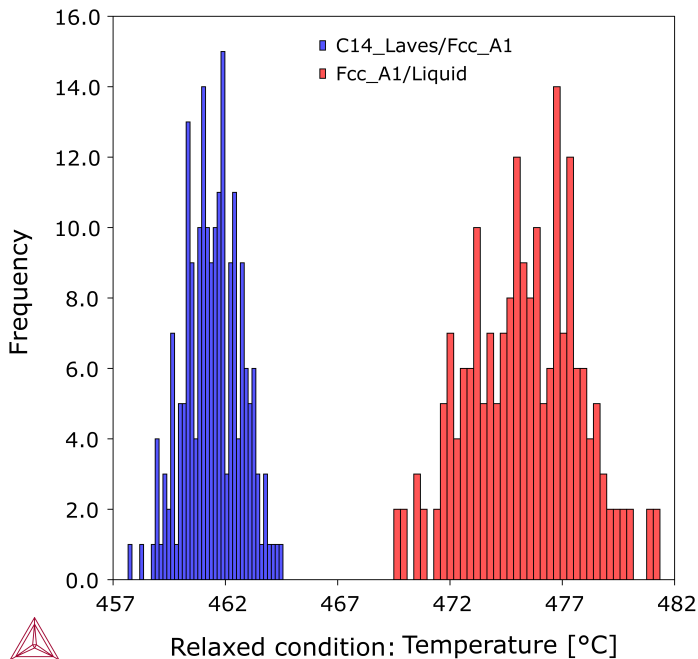


Figure 13: Uncertainty calculations for the PA Alloy using the Property Model Calculator. Temperatures are calculated at 200 compositions and the frequency of each obtained temperature is plotted.

■ Aging Treatment with the Precipitation Module (TC-PRISMA)

η' is a major strengthening precipitate in the 7000 series of alloys. After being quenched from the homogenization, the PA Alloy was aged (heating procedure: from 20 °C to 120 °C at 30 °C/h, 120 °C for 6 h, from 120 °C to 135 °C at 15 °C/h, and 135 °C for 96 h) by Marlaud [2010Mar]. [Figure 14](#) and [Figure 15](#) are from a precipitation simulation during the aging treatment. They show, respectively, the simulated solute contents in the η' precipitates and the simulated volume fraction of these precipitates.

The estimation of interfacial energy plays a central role in such a simulation. The value is estimated to be 0.045 J/m² based on a systematic consideration of all the experimental data from this alloy [2010Mar]. If considering only the simulated aging treatment, a slightly higher interfacial energy could be used and would slightly better reproduce the experimental data, but consistency is also important. There is still room for a user to refine the interfacial energy.



Read more about the [Precipitation Module \(TC-PRISMA\)](#) on our website. If you are in Thermo-Calc, press F1 to search the help to learn about the available settings included with the Add-on Module.

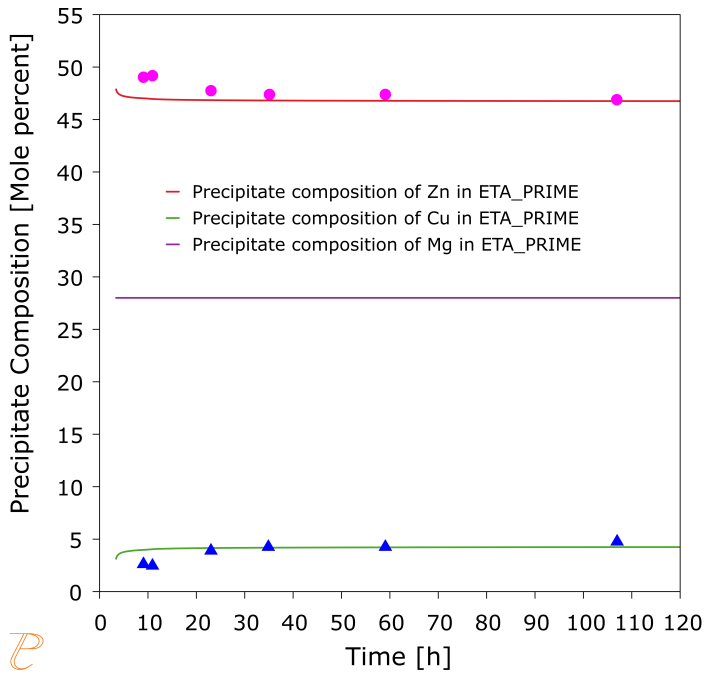


Figure 14: A simulation of the precipitation during the aging treatment showing the contents of the solutes in the η' precipitates for the PA Alloy. Curves are from the Precipitation Module (TC-PRISMA) simulations and symbols are experimental data.

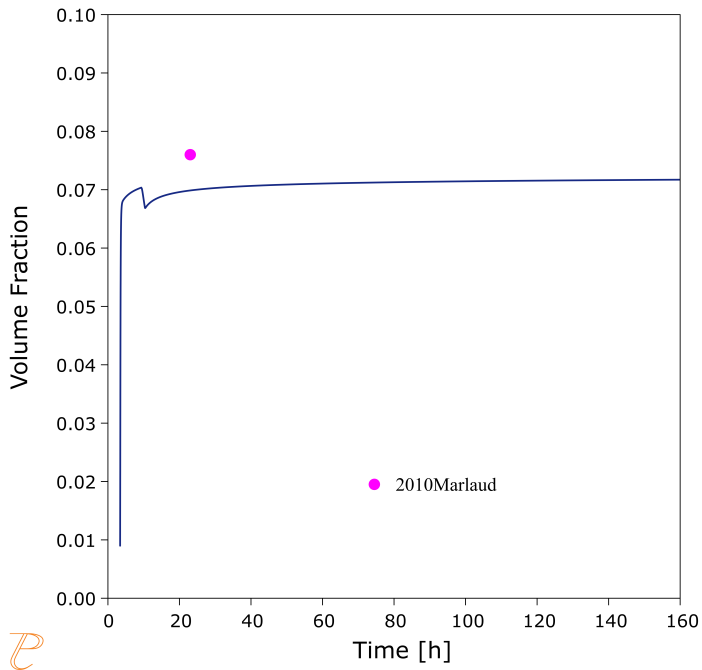


Figure 15: The simulated volume fraction of the η' precipitates in the PA Alloy during the aging treatment. Curves are from the Precipitation Module (TC-PRISMA) simulations and symbols are experimental data.

Reference

[2010Mar] T. Marlaud, A. Deschamps, F. Bley, W. Lefebvre, B. Baroux, Influence of alloy composition and heat treatment on precipitate composition in Al-Zn-Mg-Cu alloys, *Acta Mater.* 58 248-260 (2010).

Homogenization / Solution / Aging Treatment: 6005

According to this equilibrium calculation using the TCS Al-based Alloy Database (TCAL), it is impossible to attain a single (Al) phase for AA6005 alloy (Al-0.82Si-0.55Mg-0.016Cu-0.5Mn-0.2Fe, wt. %) after a solution treatment.

The temperature of 530 °C was chosen considering these factors:

- it is sufficient high to fully dissolve the Mg_2Si compound so as to maximize the amount of precipitates during aging,
- the Al₁₅Si₂M₄ phase can be dissolved to a large extent, and
- it leaves a margin to the incipient melting.

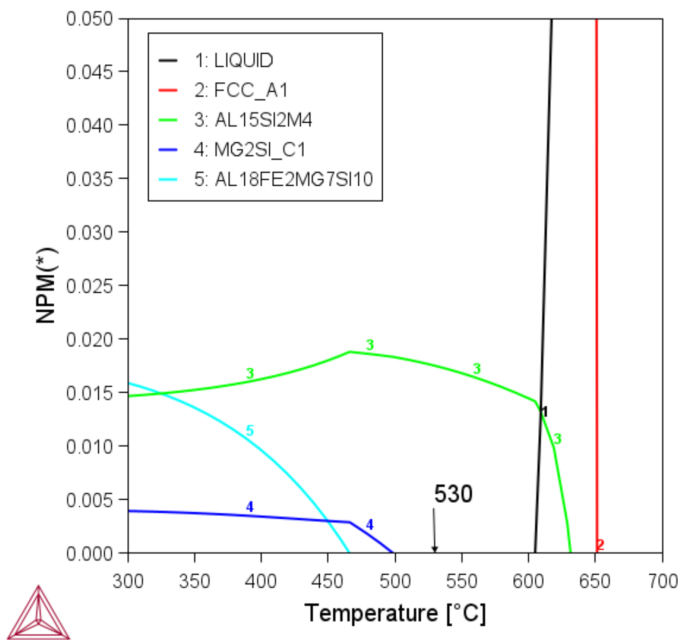


Figure 16: Equilibrium calculation for AA6005 alloy (Al-0.82Si-0.55Mg-0.016Cu-0.5Mn-0.2Fe, wt. %) after a solution treatment. See the text for discussion.

The following example is to simulate the precipitation of β'' in the (Al) matrix in the 6005 alloy. The composition of the (Al) solution, 0.562 wt.% Mg, 0.016 wt.% Cu, 0.607 wt.% Si, 0.054 wt.% Mn and 0.002 wt.% Fe, was calculated first at the solution treating temperature of 530 °C and it is slightly different from the nominal alloy composition. The figure below shows simulated mean radius and aspect ratio of β'' precipitates at 185 °C.



Read more about the [Precipitation Module \(TC-PRISMA\)](#) on our website. If you are in Thermo-Calc, press F1 to search the help to learn about the available settings included with the Add-on Module.

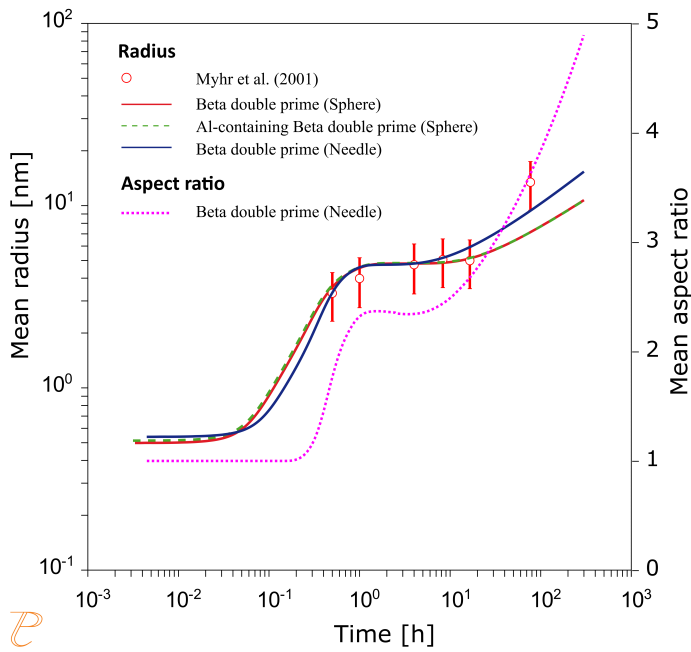


Figure 17: Simulated mean radius and aspect ratio of β'' precipitates at 185 °C. This plot uses the add-on Precipitation Module (TC-PRISMA).

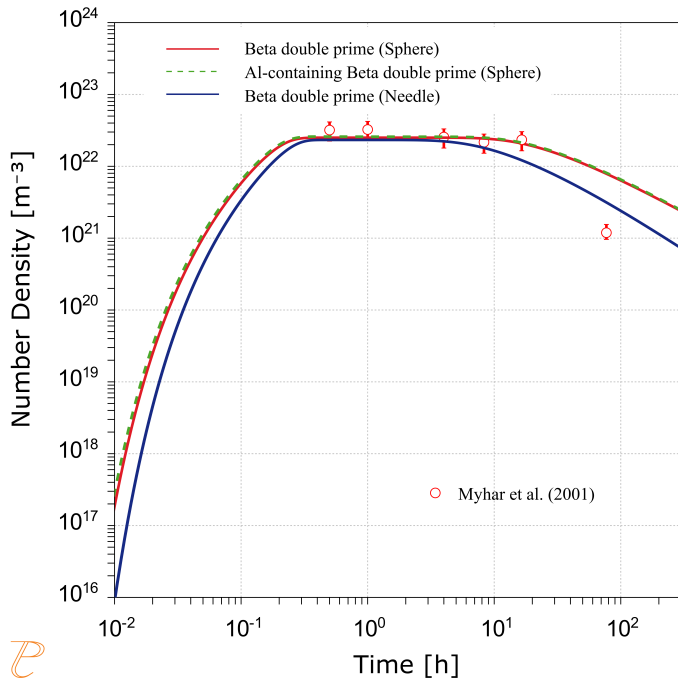


Figure 18: Simulated number density of θ'' precipitates in AA6005 alloy at 185 °C. This plot uses the add-on Precipitation Module (TC-PRISMA).

Electrical Resistivity and Thermal Conductivity

Using Thermo-Calc with the TCS AI-based Alloy Database (TCAL), you can calculate the quantities of a phase ϕ with the variables ELRS(ϕ) and THCD(ϕ), or a system (i.e. alloy) with ELRS and THCD. You can also calculate the derived quantities, i.e. electrical conductivity (ELCD), thermal resistivity (THRS) and thermal diffusivity (THDF) in a similar way.

The database includes electrical resistivity and thermal conductivity starting with version 7 (TCAL7).



You can find information on our website about the [properties that can be calculated](#) with Thermo-Calc and the Add-on Modules. Additional resources are added on a regular basis so keep checking back or [subscribe to our newsletter](#).

Wrought Al Alloys

This example compares the calculated ELRS ([Figure 19](#)) and THCD ([Figure 20](#)) with tabulated data for typical Al alloys after “O” heat treatments. For each alloy, an equilibrium calculation is first performed at 350 °C (assumed annealing temperature), so phases that are present, and their fractions and compositions are obtained with Thermo-Calc. Then the temperature is changed to 25 °C (measuring temperature), and the value of ELRS is directly retrieved without equilibrium-computing.



For alloys produced with other treatments, sometimes you have to take into account impacts of deformations and precipitations, and so forth. For as-cast alloys, you can use Scheil simulations (with or without back diffusion) to predict the phases, as well as the fractions and compositions, and then evaluate ELRS and THCD appropriately.



Read more about [Scheil Solidification Simulations](#) on our website, including [how to select the right model for your simulation](#). If you are in Thermo-Calc, press F1 to search the help to learn about using Scheil.

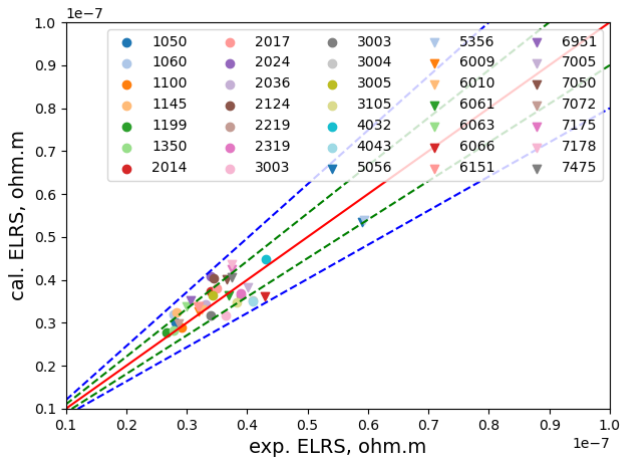


Figure 19: Compares the calculated ELRS with tabulated data for 35 wrought Al alloys after "O" heat treatments. The calibration is assumed to be proportional to the total fraction of grain boundary phases with a coefficient of $+4.83e-8$ ohm.m. The red solid line indicates where calculated values are equal to experimental data. The blue dashed lines mark the limits for 20 % deviations and the green dashed lines for 10 % deviations. The data are from ASM [1990].

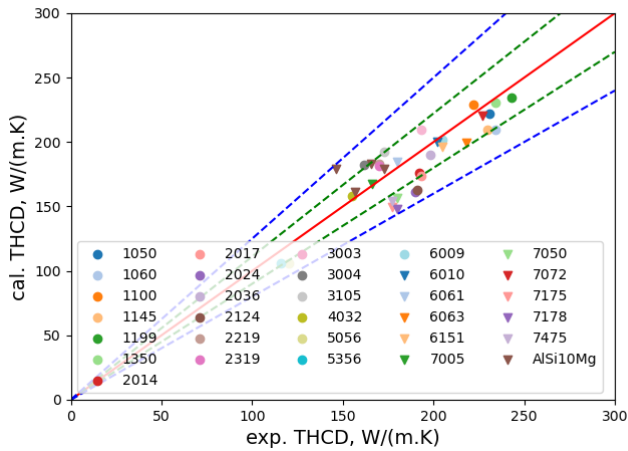


Figure 20: Compares the calculated THCD with tabulated data for 31 Al alloys after "O" heat treatments. The calibration of THCD is based on that of ELRS, assuming they obey the Wiedemann-Franz Law. The red solid line indicates where calculated values are equal to experimental data. The blue dashed lines mark the limits for 20 % deviations and the green dashed lines for 10 % deviations. The data are from ASM [1990].

References

- [1972Ho] C. Y. Ho, R. W. Powell, P. E. Liley, Thermal Conductivity of the Elements. *J. Phys. Chem. Ref. Data.* 1, 279–421 (1972).
- [1983Ho] C. Y. Ho, M. W. Ackerman, K. Y. Wu, T. N. Havill, R. H. Bogaard, R. A. Matula, S. G. Oh, H. M. James, Electrical Resistivity of Ten Selected Binary Alloy Systems. *J. Phys. Chem. Ref. Data.* 12, 183–322 (1983).
- [1990ASM] Properties and selection: nonferrous alloys and special-purpose materials, in *ASM Handbook* 10th edition, Metals Handbook. ASM International, 1990.
-

Surface Tension of Two Alloys: A356 and Alufont-47

The surface tension thermophysical property data is included with the TCS AI-based Alloy Database (TCAL) as of version 7 (TCAL7).

For more information about the various thermophysical, thermomechanical, and properties models, and when in Thermo-Calc, press F1 to search the online help. The details are found under a *General Reference* section.



You can find information on our website about the [properties that can be calculated](#) with Thermo-Calc and the Add-on Modules. Additional resources are added on a regular basis so keep checking back or [subscribe to our newsletter](#).

A356 Alloy

The following compares the calculated surface tension of an A356 alloy as a function of Mg content with experimental data that are measured under hydrogen and vacuum environment and with and without Sr.

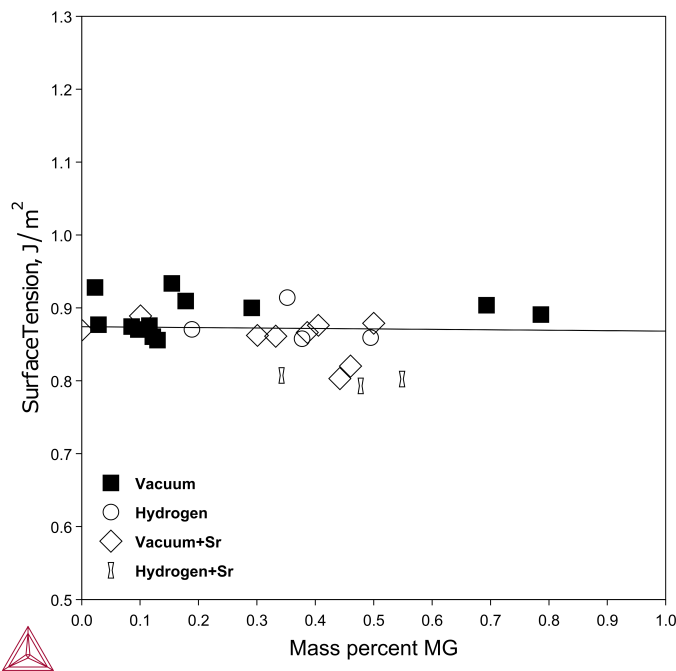


Figure 21: The surface tension of A356 + Mg alloys with and without Sr at 630 °C. The experimental data are taken from [1999Ans].

Alufont-47 Alloy

AlCu₄TiMg, also known as Alufont-47, is a lightweight alloy which is commonly used in the automotive and aerospace industries. Plevachuk et al. [2020Ple] have measured some important thermophysical properties of this alloy including the surface tension, density, and thermal conductivity. The surface tension was measured with an oscillating drop technique using an electromagnetic levitation apparatus. The composition of the alloy used in their measurements in at% is:

Sample	Cu	Mg	Si	Ti	Fe	Mn	Zn	Al
Alufont-47	1.9	0.4	0.1	0.2	<0.1	<0.1	<0.1	remainder

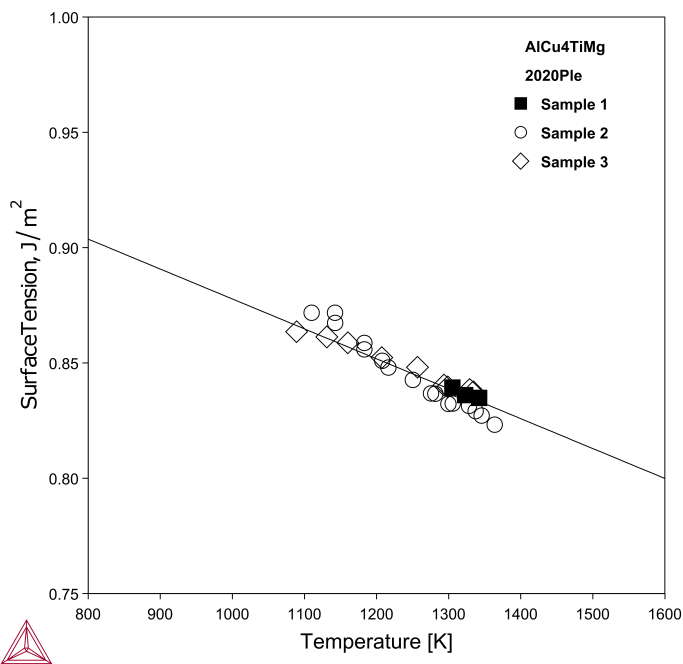


Figure 22: Calculated surface tension of AlCu₄TiMg alloy along with experimental data from [2020Ple].

Gancarz et al. [2021Gan] measured the surface tension of Al-5Mg-0.2Sc with addition of 3 and 6 wt% Li by means of discharge crucible method.

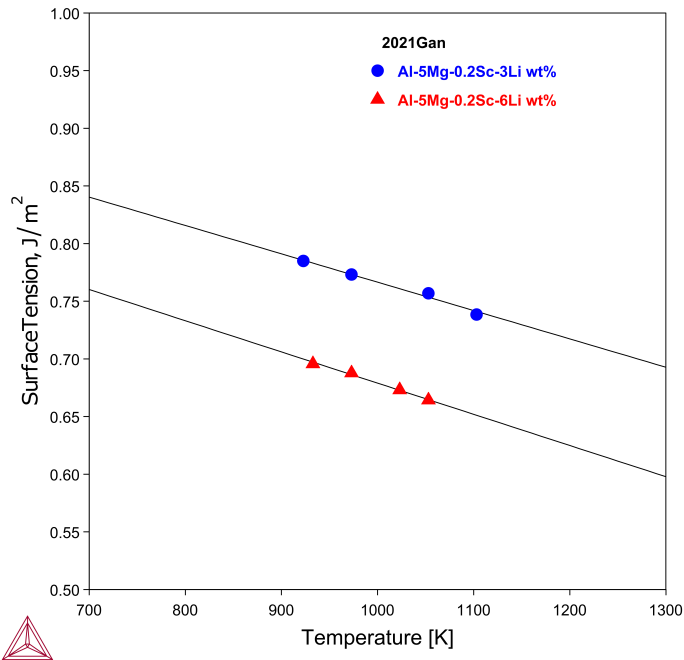


Figure 23: Calculated surface tension of two Al-Mg-Sc-Li alloys compared with experimental data from [2021Gan].

References

- [1999Ans] J. P. Anson, R. A. L. Drew, J. E. Gruzleski, The surface tension of molten aluminum and Al-Si-Mg alloy under vacuum and hydrogen atmospheres. *Metall. Mater. Trans. B.* 30, 1027–1032 (1999).
- [2020Ple] Y. Plevachuk, V. Sklyarchuk, G. Pottlacher, T. Leitner, P. Švec Sr., P. Švec, L. Orovck, M. Dufanets, A. Yakymovych, The liquid AlCu4TiMg alloy: thermophysical and thermodynamic properties. *High Temp. - High Press.* 49, 61–73 (2020).
- [2021Gan] T. Gancarz, A. Dobosz, A.-A. Bogno, G. Cempura, N. Schell, R. Chulist, H. Henein, Characterization of rapidly solidified Al-Mg-Sc alloys with Li addition. *Mater. Charact.* 178, 1044–5803 (2021).

Viscosity of Various Alloys

The viscosity thermophysical property data is included with the TCS AI-based Alloy Database (TCAL) as of version 7 (TCAL7).

For more information about the various thermophysical, thermomechanical, and properties models, and when in Thermo-Calc, press F1 to search the online help. The details are found under a *General Reference* section.



You can find information on our website about the [properties that can be calculated](#) with Thermo-Calc and the Add-on Modules. Additional resources are added on a regular basis so keep checking back or [subscribe to our newsletter](#).

A201, A319, and A356 Alloys

Wang and Overfelt [2002Wan] measured the viscosity of pure Al and A201, A319, and A356 alloys with oscillating cup viscometer.

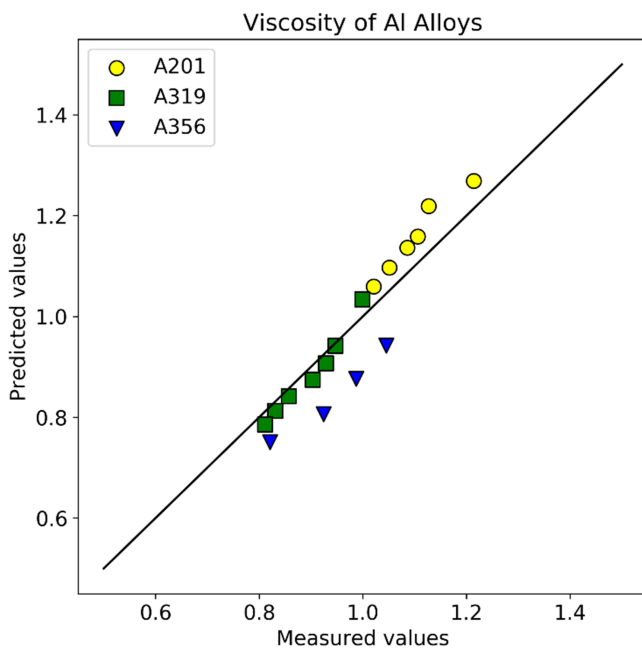


Figure 24: The measured values of the viscosity of A201, A319, and A356 alloys are compared with the predicted values. The experimental data are from [2002Wan].

Al-Mg-Sc-Li Alloys

Gancarz et al. [2021Gan] measured the viscosity of Al-5Mg-0.2Sc with addition of 3 and 6 wt% Li by means of discharge crucible method.

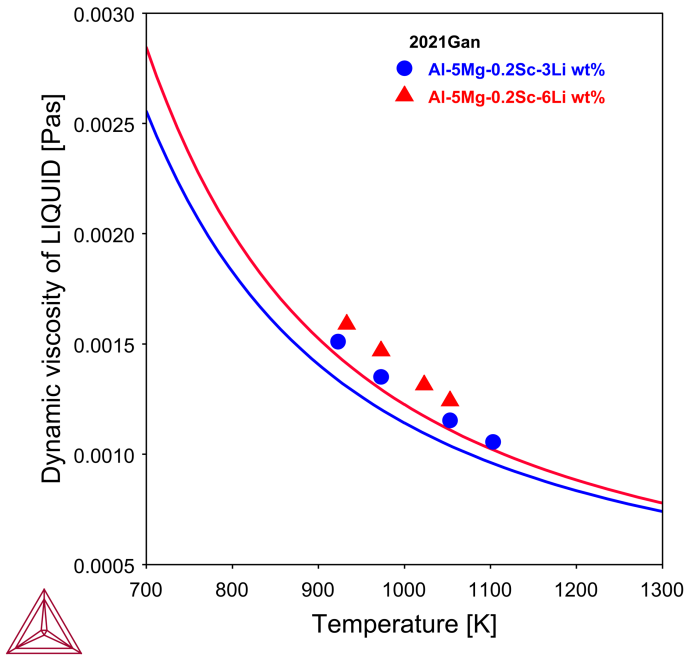


Figure 25: Calculated dynamic viscosity of two Al-Mg-Sc-Li alloys compared with experimental data from [2021Gan].

References

- [2002Wan] D. Wang, R. A. Overfelt, Oscillating Cup Viscosity Measurements of Aluminum Alloys: A201, A319 and A356. *Int. J. Thermophys.* 23, 1063–1076 (2002).
- [2021Gan] T. Gancarz, A. Dobosz, A.-A. Bogno, G. Cempura, N. Schell, R. Chulist, H. Henein, Characterization of rapidly solidified Al-Mg-Sc alloys with Li addition. *Mater. Charact.* 178, 1044–5803 (2021).

TCAL Calculation Examples



Some diagrams are calculated with earlier versions of the database. Negligible differences might be observed if these are recalculated with the most recent version. The diagrams are updated when there are considerable or significant improvements.

In this section:

Al-Li	34
Al-Er	36
Al-Fe-Si	37
Al-Mn-Si	39
Al-Fe-Mn-Si	40
Al-Cu-Mg-Zn	41
Al-Cu-Mg-Si	43
Minor Alloying Elements	44
Al-Ce-Mg	46
Molar Volume and Related Examples	47
Metastable Phases / Precipitates	50
Electrical Resistivity and Thermal Conductivity	52
Viscosity: Al-Cu and Cu-Al-Si	57
Surface Tension: Al-Cu and Ag-Al-Cu	59

Al-Li

Lithium (Li) is an important alloying element to some 8000 series (Al-Li based) and 2000 series (Al-Cu-Li-based) of aluminum alloys. In this example using the TCS Al-based Alloy Database (TCAL), the AL1LI2 stable phase is included in the equilibrium phase diagram (Figure 26) and the L1₂-type metastable precipitate Al₃Li (named as AL₃X, X=Er, Li, Sc, Ti, Zr) is modeled.

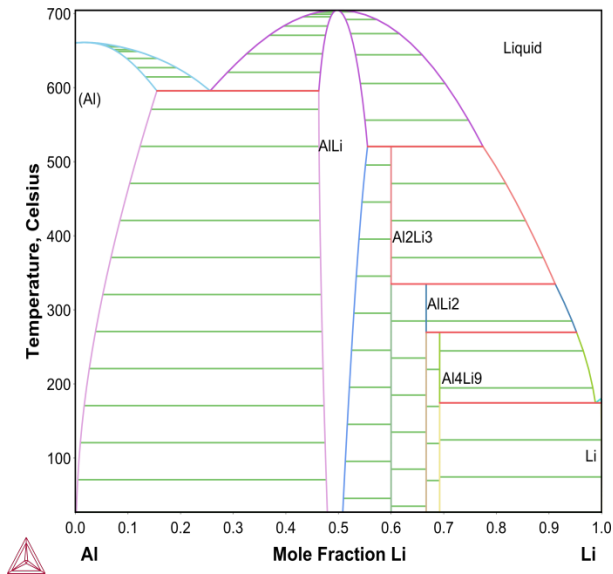


Figure 26: Calculated Al-Li phase diagram [1989Sau; 2012/2017Che].

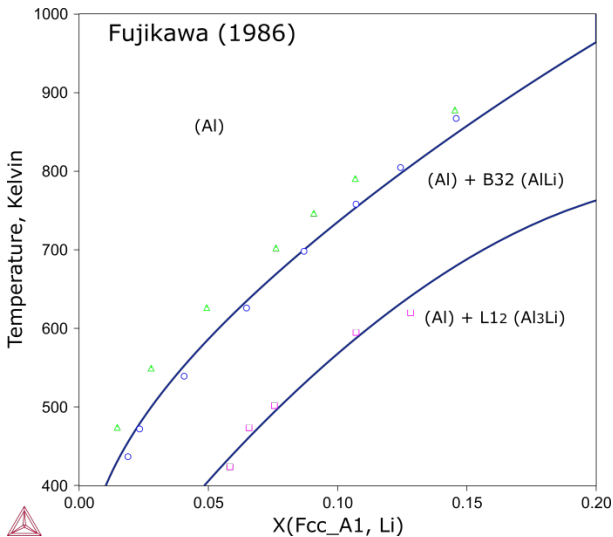


Figure 27: Calculated (Al) solvi in the Al-Li system (references from Figure 26) in comparison with the data from [1986Fuj].

References

- [1986Fuj] S. Fujikawa, Solvuses of delta' phase (Al₃Li) and delta phase (AlLi) in Al-Li alloys. J. Japan Inst. Light Met. 36, 771–777 (1986).
- [1989Sau] N. Saunders, Calculated stable and metastable phase equilibria in Al-Li-Zr alloys. Zeitschrift fur Met. 80, 894–903 (1989).
- [2012/2017Che] H.-L. Chen, Modeling of the AlLi₂ and Al₃Li phases in the Al-Li binary system, unpublished work, 2012/2017.
-

Al-Er

As a rare earth element, Er recently attracted research interest. The Er addition forms the $L1_2$ -type precipitate Al_3Er (named as Al_3X , $X=Er, Li, Sc, Ti, Zr$). This is a stable phase and its melting temperature is higher than that of Al.

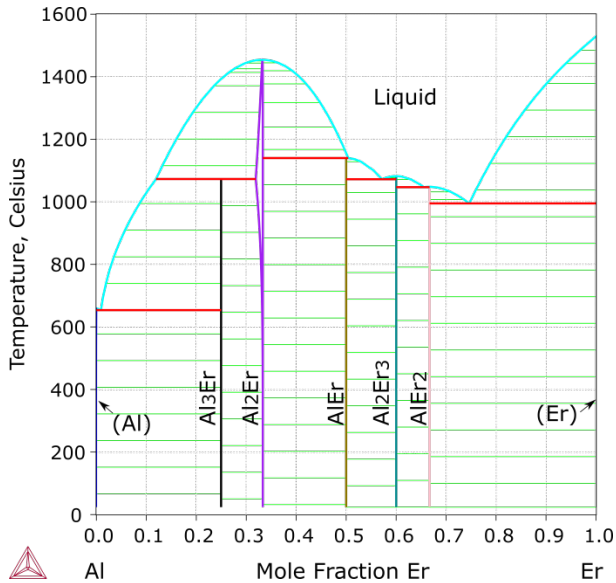


Figure 28: Calculated Al-Er phase diagram, where the Er solubility in (Al) is evaluated [2017Che].

Reference

[2017Che] H.-L. Chen, Thermodynamic modeling of the Er-X ($X = Ag, Al, Fe, Si, Zr$) binary and Al-Er-X ($X=Cu, Fe, Mg$) ternary systems (Stockholm, Sweden, 2017), unpublished.

Al-Fe-Si

Al-Fe-Si is a core system, as Fe and Si exist in all aluminum alloys either as a common alloying element or an inevitable impurity. The two Al-Fe-Si compounds, τ_5 : $\alpha\text{-Al}_8\text{Fe}_2\text{Si}$ and τ_6 : $\beta\text{-Al}_9\text{Fe}_2\text{Si}_2$, are frequently observed in aluminum alloys. Additionally, τ_4 may form in high-Si aluminum alloys.

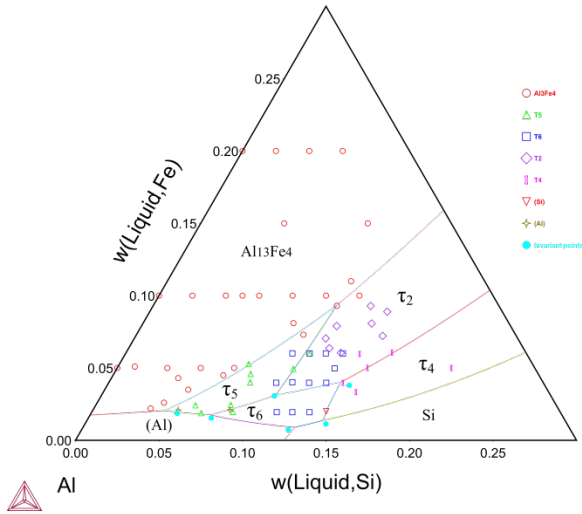


Figure 29: Calculated Al-Fe-Si liquidus projection (τ_5 : $\alpha\text{-AlFeSi}$; τ_6 : $\beta\text{-AlFeSi}$), (a) in the Al-rich corner. The invariant points are from [2004Pon; 2004Bos]. The remaining data are from [1940Tak; 1967Mun; 1988Zak].

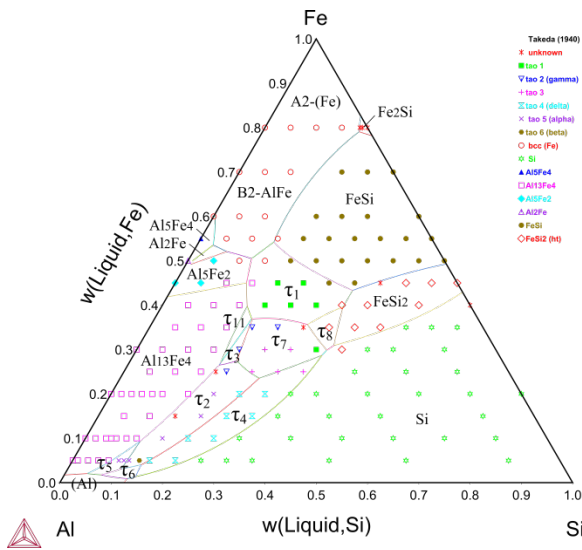


Figure 30: Continuing from [Figure 29](#) this is over the entire compositional range, with the data from [1940Tak].

References

- [1940Tak] S. Takeda, K. Mutuzaki, The equilibrium diagram of the Fe–Al–Si system. *Tetsu-to-Hagane*. 26, 335–361 (1940).
- [1967Mun] D. Munson, A Clarification of the Phases Occurring in Aluminium-Rich Aluminium-Iron-Silicon Alloys, with Particular Reference to the Ternary Phase α -AlFeSi. *J. Inst. Met.* 95, 217–219 (1967).
- [1988Zak] A. M. Zakharov, I. T. Gulman, A. A. Arnold, Y. A. Matsenko, Phase diagram of the Aluminium-Silicon-Iron system in the concentration range of 10-14% Si and 0-3% Fe. *Russ. Metall.* 3, 177–180 (1988).
- [2004Bos] F. Bosselet, S. Pontevichi, M. Sacerdote-Peronnet, J. C. Viala, Experimental measurement of the Al-Fe-Si isothermal section at 1000 K. *J. Phys. IV.* 122, 41–46 (2004).
- [2004Pon] S. Pontevichi, F. Bosselet, F. Barbeau, M. Peronnet, J. C. Viala, Solid-liquid phase equilibria in the Al-Fe-Si system at 727 °C. *J. Phase Equilibria Diffus.* 25, 528–537 (2004).
-

Al-Mn-Si

Al-Mn-Si is another core system to aluminum alloys. Mn is often added to suppress the formation of the detrimental τ_5 : $\alpha\text{-Al}_8\text{Fe}_2\text{Si}$ and τ_6 : $\beta\text{-Al}_9\text{Fe}_2\text{Si}_2$, via forming the $\alpha\text{-AlMnSi}$ phase (named as AL15SI2M4, M=Cr, Fe, Mn, Mo). The $\alpha\text{-AlMnSi}$ phase originates in the Al-Mn-Si ternary system and extends towards the Al-Fe-Si system via the substitution of Fe for Mn. The substitution of Cr and Mo for Mn is also modeled in the TCS Al-based Alloy Database (TCAL).

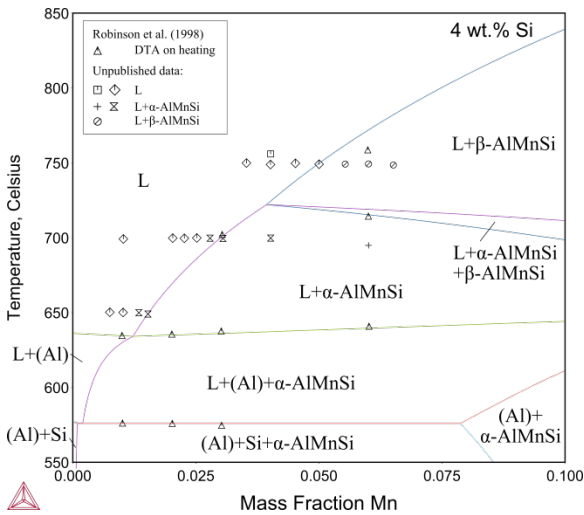


Figure 31: Al-Mn-Si vertical section at 4 wt. % Si ($\beta\text{-AlMnSi}$: τ_8 ; $\alpha\text{-AlMnSi}$: τ_9) [2014Che].

Reference

[2014Che] H. Chen, Q. Chen, Y. Du, J. Bratberg, A. Engström, Update of Al-Fe-Si, Al-Mn-Si and Al-Fe-Mn-Si thermodynamic descriptions - TNMSC. Chinese J. Nonferrous Met. 24, 2041–2053 (2014).

Al-Fe-Mn-Si

Adding a small amount of Mn may promote the formation of the α -AlMnSi phase (named as AL15SI2M4, M=Cr, Fe, Mn, Mo). In fact, it competes with Al-Fe-Si compounds and forms during the casting of a wide variety of aluminum alloys.

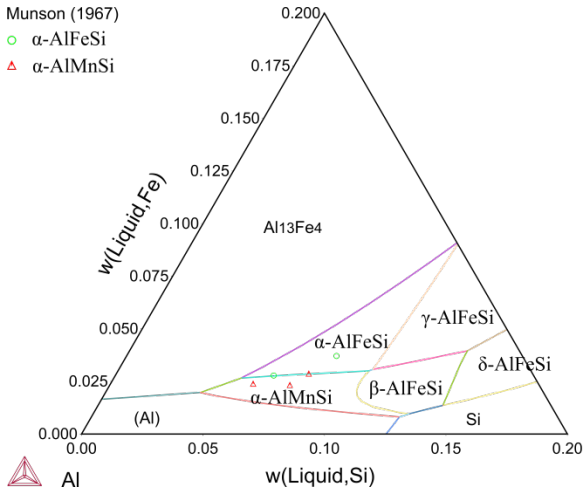


Figure 32: Al-Fe-Mn-Si liquidus surface at 0.3 wt. % Mn. (α -AlFeSi: τ_5 ; β -AlFeSi: τ_6 ; γ -AlFeSi: τ_2 ; δ -AlFeSi: τ_4 ; α -AlMnSi: τ_9) [2014Che].

Reference

[2014Che] H. Chen, Q. Chen, Y. Du, J. Bratberg, A. Engström, Update of Al-Fe-Si, Al-Mn-Si and Al-Fe-Mn-Si thermodynamic descriptions - TNMSC. Chinese J. Nonferrous Met. 24, 2041–2053 (2014).

Al-Cu-Mg-Zn

The Al-Cu-Mg-Zn quaternary system is the basis of the 7000 series of wrought Al alloys. The formation of the major compounds such as Al₂Cu, S_PHASE, T_PHASE, V_PHASE, and M (aka. η, modeled as C14_LAVES) is essentially determined by the quaternary phase equilibria. Small additions of other alloying elements such as Fe and Mn may form additional compounds, while the formation of those major compounds is barely affected. The 7000 series are heat treatable and a typical solution treatment is performed around 460 °C.

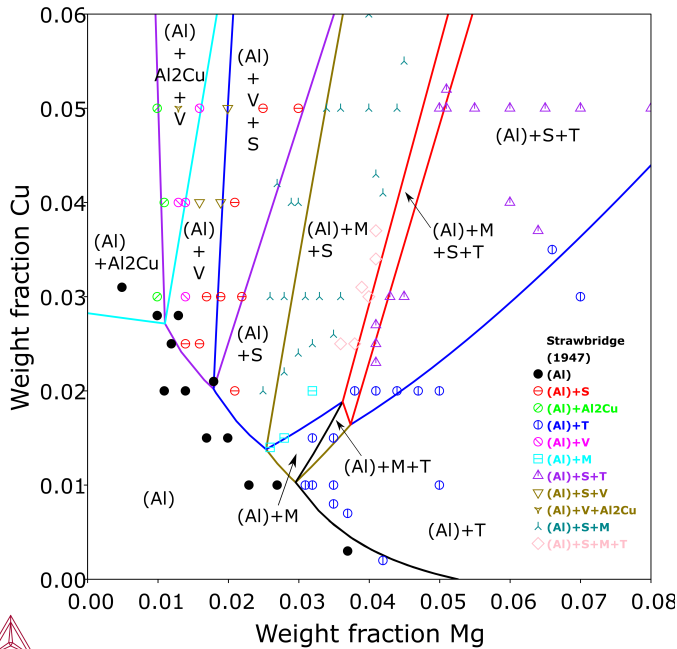


Figure 33: Calculated isothermal sections of the Al-Cu-Mg-Zn system at 460 °C: at 8 wt. % Zn [2012Che] with experimental data from [1948Str].

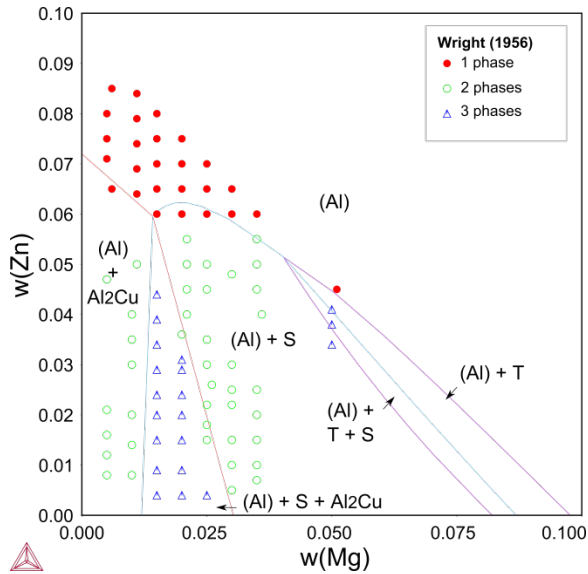


Figure 34: Calculated isothermal sections of the Al-Cu-Mg-Zn system at 90 wt.% Al with experimental data from [1956Wri].

References

- [1948Str] D. J. Strawbridge, A. Little, The Constitution of Aluminium Copper Magnesium Zinc Alloys At 460 °C. *J. Inst. Met.* 74, 191–225 (1948).
- [1956Wri] E. H. Wright, Equilibrium relations at 460 °C in aluminum-copper-magnesium-zinc alloys of high purity (Internal Report 13–56-EC2, Aluminum Research Laboratories, Aluminum Company of America, 1956).
- [2012Che] H.-L. Chen, Thermodynamic assessment of the Al-Cu-Mg-Zn(-Fe) and Al-Cu-Mg-Si multicomponent alloy systems (Stockholm, Sweden, 2012), unpublished work.

Al-Cu-Mg-Si

Aluminum alloys based in the quaternary system Al-Cu-Mg-Si are widely used, e.g. in the automotive and aerospace industry. The Al-Cu-Mg-Si family of aluminum alloys may exist either as a 6xxx or a 2xxx alloy. These alloys have distinctive properties in part due to the occurrence of the Q phase, which is stable as a quaternary compound.

This TCS Al-based Alloy Database (TCAL) vertical section example shows satisfactory agreements between experimental data and calculations on phase equilibria at 60 wt.% Al, 8 wt.% Si, involving Q, θ (Al₂Cu), liquid, β (Mg₂Si), (Si), S_PHASE, and T_PHASE.

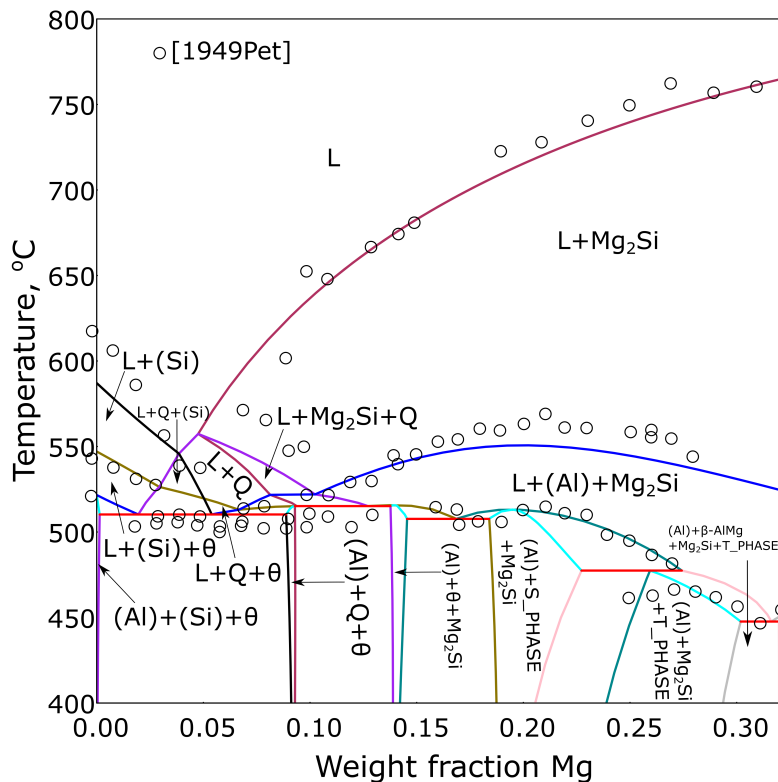


Figure 35: Calculated vertical section at 60 wt.% Al, 8 wt.% Si with experimental data from [1949Pet].

Reference

[1949Pet] D. A. Petrov, N. D. Nagorskaya, Constitution diagram of the aluminum-copper-magnesium-silicon system. Zhurnal Obs. Khimii 19, 1994–2037 (1949).

Minor Alloying Elements

Al-Cr

Many minor alloying elements and related systems are modeled in the TCS Al-based Alloy Database (TCAL). Cr is one of them. In the first place, and in order to reliably predict the formation of relevant compounds, the solubility of these elements in the melt and the (Al) solid solution must be well modeled.

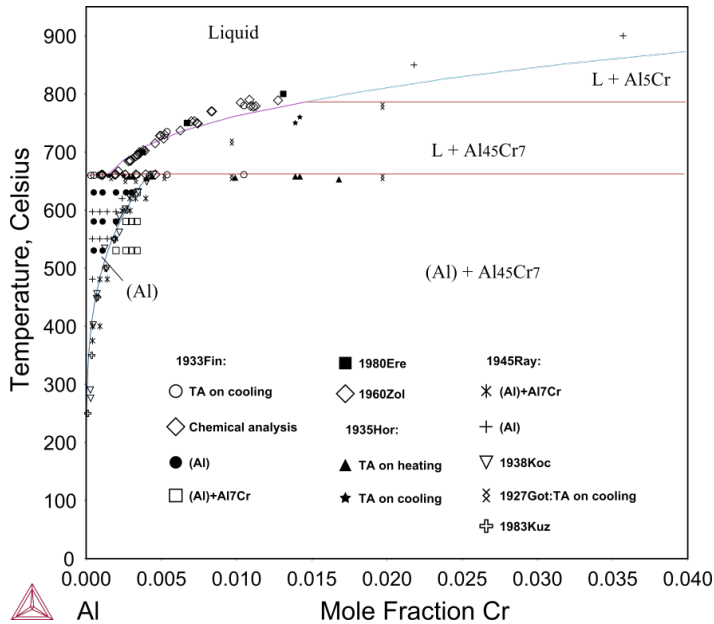


Figure 36: Calculated Al-rich Al-Cr binary phase diagram with experimental data.

Al-Sn-Zn

Sn is an important minor alloying element in aluminum alloys. Many Sn-containing systems have been assessed since TCS Al-based Alloy Database version 5 (TCAL5).

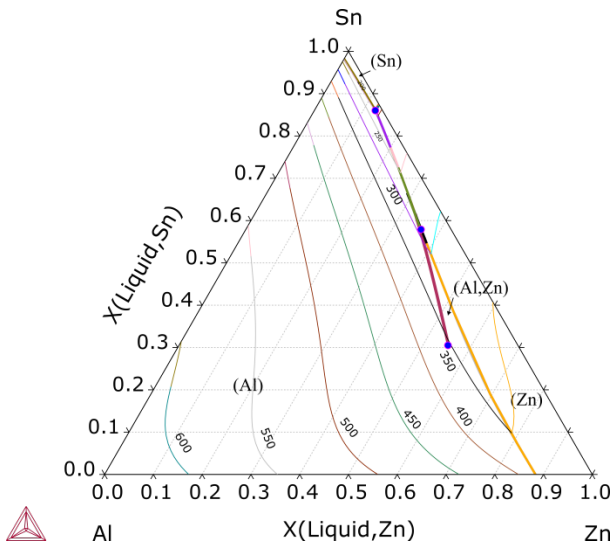


Figure 37: Al-Sn-Zn liquidus surface projection with isotherms [2017Che].

Reference

[2017Che] H.-L. Chen, Thermodynamic modeling of the Al-Sn-X (X = Cd, Cu, In, Si, Zn) ternary systems (Stockholm, Sweden, 2017), unpublished work.

Al-Ce-Mg

High-performance and lightweight aluminum-cerium alloys are recently reported to be potential candidates for high-temperature applications [2017Sim]. Ce and many related systems have been added since TCS Al-based Alloy Database version 5 (TCAL5).

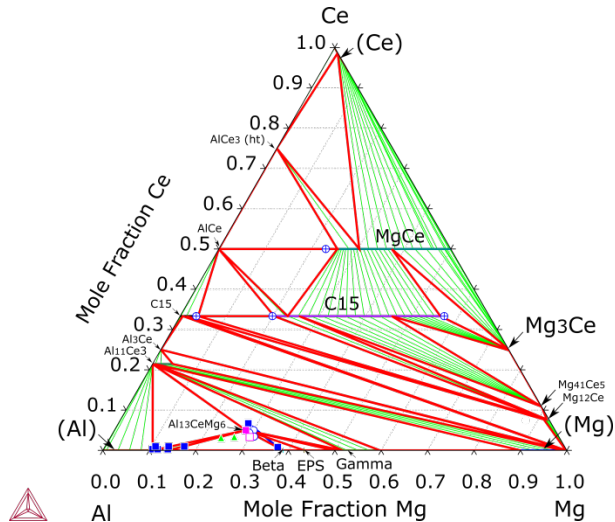


Figure 38: Al-Ce-Mg isothermal section at 400 °C [2017Che].

References

- [2017Che] H.-L. Chen, Thermodynamic modeling of the Al-Ce-X (X = Cr, Fe, Mg, Mn, Ni, Si) ternary systems (Stockholm, Sweden, 2017), unpublished.
- [2017Sim] Z. C. Sims, O. R. Rios, D. Weiss, P. E. A. Turchi, A. Perron, J. R. I. Lee, T. T. Li, J. A. Hammons, M. Bagge-Hansen, T. M. Willey, K. An, Y. Chen, A. H. King, S. K. McCall, High performance aluminum–cerium alloys for high-temperature applications. *Mater. Horizons*. 4, 1070–1078 (2017).

Molar Volume and Related Examples

The TCS Al-based Alloy Database (TCAL) contains a molar volume and thermal expansion coefficients of all phases starting with version 2 (TCAL2).



You can find information on our website about the [properties that can be calculated](#) with Thermo-Calc and the Add-on Modules. Additional resources are added on a regular basis so keep checking back or [subscribe to our newsletter](#).

The database can be used for:

- Calculating the molar volume (and thus the density) of the (Al) solid solution ([Figure 39](#)).
- Predicting the casting shrinkage of aluminum alloys ([Figure 40](#)).
- Calculating the thermal expansion ([Figure 41](#))

Al-X (X=Li, Mg, Si, Zn) Molar Volumes

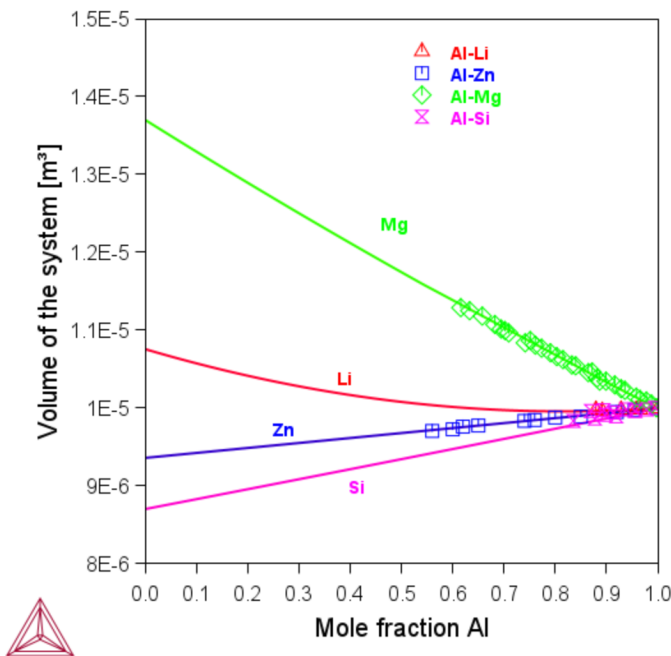


Figure 39: Calculated molar volumes of the Al-X (X=Li, Mg, Si, Zn) fcc_A1 phase.

Al and Al-Si Alloy Densities

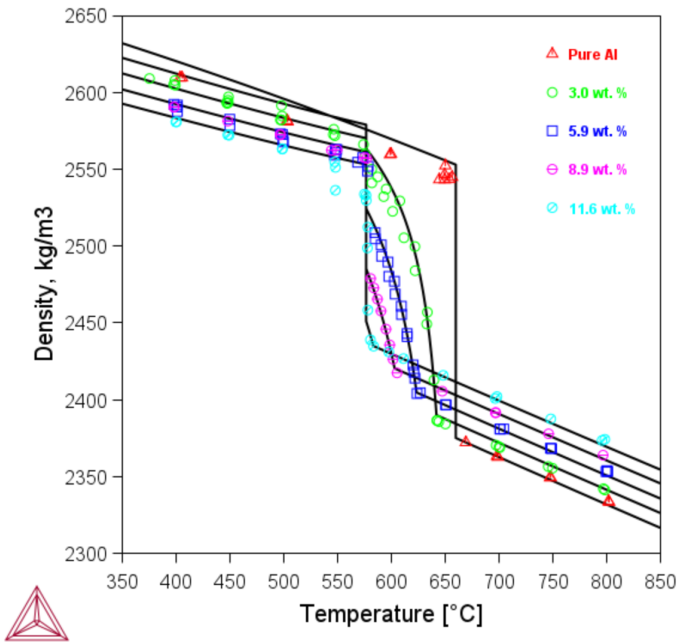


Figure 40: Calculated densities of pure Al and Al-Si alloys versus the temperature, in comparison with experimental data from [2001Mag].

Al-Sc, Al-Ti, and Al-Zr Thermal Expansivity

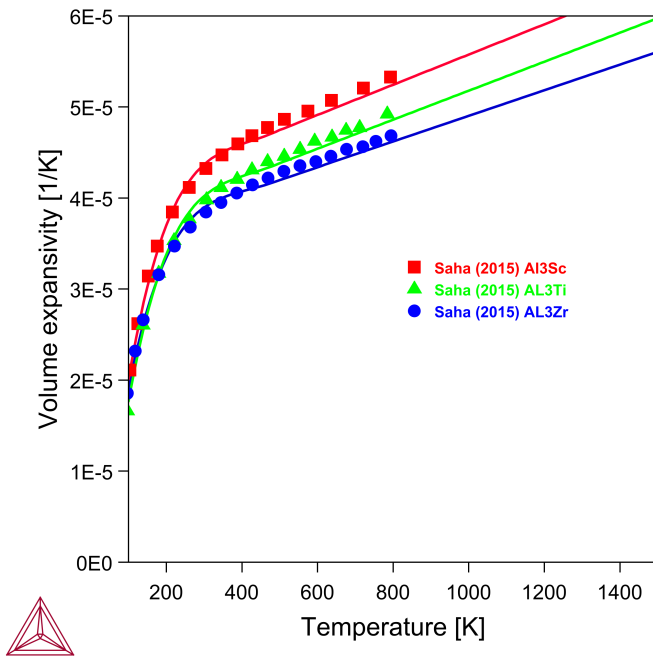


Figure 41: Calculated volume thermal expansivity for Al_3Sc , Al_3Ti , and Al_3Zr [2017Che].

References

- [2001Mag] T. Magnusson, L. Arnberg, Density and solidification shrinkage of hypoeutectic aluminum-silicon alloys. *Metall. Mater. Trans. A.* 32, 2605–2613 (2001).
- [2017Che] H.-L. Chen, Thermodynamic modeling of phase equilibria and molar volume in the Sc-Ti, Al-Sc-Si, Al-Sc-Ti, Al-Sc-Zr and Al-Si-Ti systems (Stockholm, Sweden, 2017), unpublished work.
-

Metastable Phases / Precipitates

Most important precipitates that form during aging treatments and casting of aluminum alloys are metastable, except for a few such as Al_3Sc and Al_3Er (both modeled as Al_3X). This example uses the TCS Al-based Alloy Database (TCAL).

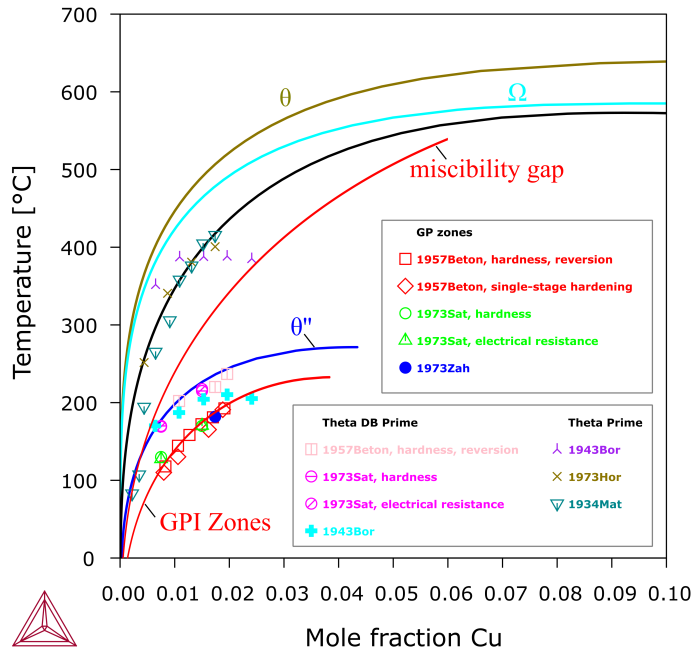


Figure 42: Calculated Al-Cu (Al) solvus curves equilibrated with θ , Ω , θ' , θ'' (or GPII zones) and GPI zones, respectively. A metastable miscibility gap of fcc_A1 is shown. The GPI zones are modeled as the second composition set of fcc_A1, i.e. fcc_A1#2. It is assumed that experimentally observed GPI zones are usually tiny (say < 3 nm), so the interfacial and elastic energy are considered. The line for GPI zones is calculated with adding +800 J/mole-atoms to the energy of fcc_A1#2 [2014Che].

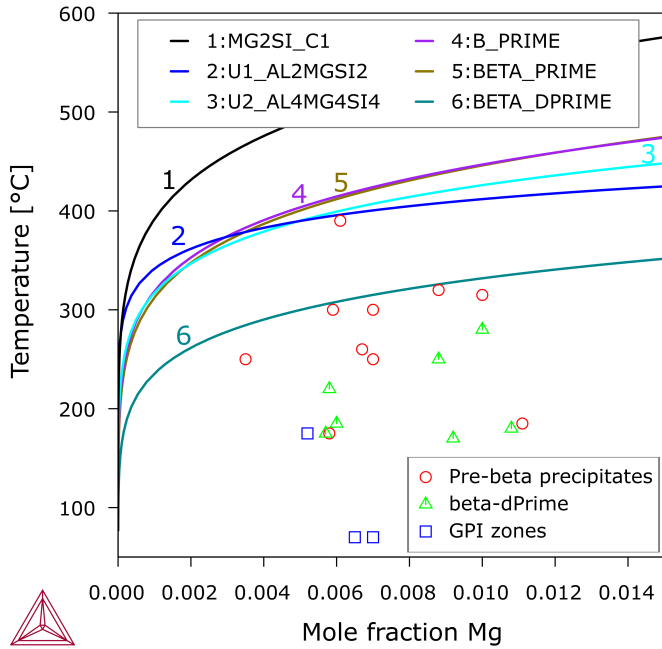


Figure 43: Calculated fcc_A1 solvi in alloys at 0.73 at.% Si and varying Mg content, relative to different Al-Mg-Si precipitates, including the stable β - Mg_2Si phase, pre- β precipitates (β' , U1, U2 and B') and the pre- β' precipitate, i.e. β'' . The symbols indicate certain precipitates have been experimentally observed in alloys of given compositions and aged at given temperatures [2014Che].

Reference

[2014Che] H.-L. Chen, Thermodynamic modeling of metastable precipitate phases in Al-Cu, Al-Fe, Al-Mg-Si, and Al-Mg-Zn based alloys (Stockholm, Sweden, 2014), unpublished work.

Electrical Resistivity and Thermal Conductivity

Electrical resistivity and thermal conductivity of Al alloys are of great importance since the alloys are widely used as electrical cables and radiators in cars and refrigerators. Moreover, thermal conductivity data are needed for designing processes in additive manufacturing.

Using Thermo-Calc with the TCS Al-based Alloy Database (TCAL), you can calculate the quantities of a phase ϕ , with the variables ELRS(ϕ) and THCD(ϕ) or a system (i.e. alloy), with ELRS and THCD. You can also calculate derived quantities, including electrical conductivity (ELCD), thermal resistivity (THRS) and thermal diffusivity (THDF) in a similar way.

For more information about the various thermophysical, thermomechanical, and properties models, and when in Thermo-Calc, press F1 to search the online help. The details are found under a *General Reference* section.

The database includes electrical resistivity and thermal conductivity starting with version 7 (TCAL7).



You can find information on our website about the [properties that can be calculated](#) with Thermo-Calc and the Add-on Modules. Additional resources are added on a regular basis so keep checking back or [subscribe to our newsletter](#).

Al: Electrical Resistivity

In this example, the theoretical model and its parameters is first fitted to the data from [1983Ho] and extrapolated to high temperatures, i.e. 2000 K. A polynomial is then fitted to the data and the extrapolated values and the resulting parameters are stored in the database. Such treatments benefit from the simplicity using polynomials and guarantee the reliability for the extrapolation.

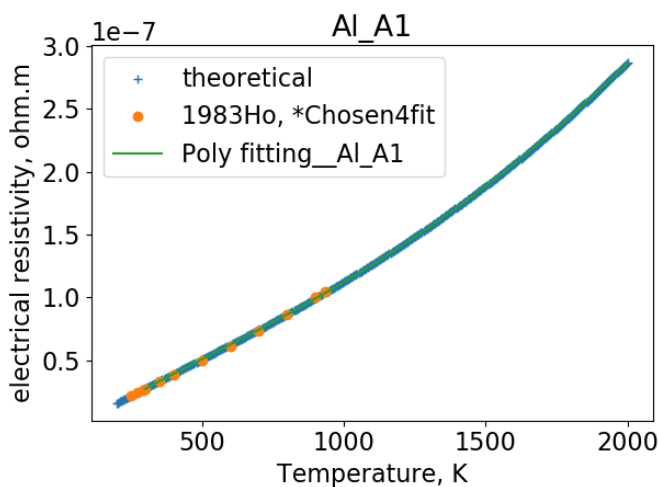


Figure 44: The modeling of electrical resistivity (ELRS) of FCC_A1 Al.

Ni: Electrical Resistivity and Thermal Conductivity

In [Figure 45](#) (left), the calculated electrical resistivity of pure Ni is compared with experimental data from Chu et al. [1982Chu]. There is a magnetic contribution to the resistivity, which is described with

$$\rho_m = \rho_{spd} \cdot \left(1 - e^{\left(-\frac{3}{2} \left(\frac{T}{T_c} \right)^3 \right)} \right)$$

that is implemented in Thermo-Calc. In [Figure 45](#) (right) the plot compares the calculated thermal conductivity of pure Ni with experimental data from Ho et al. [1972Ho].

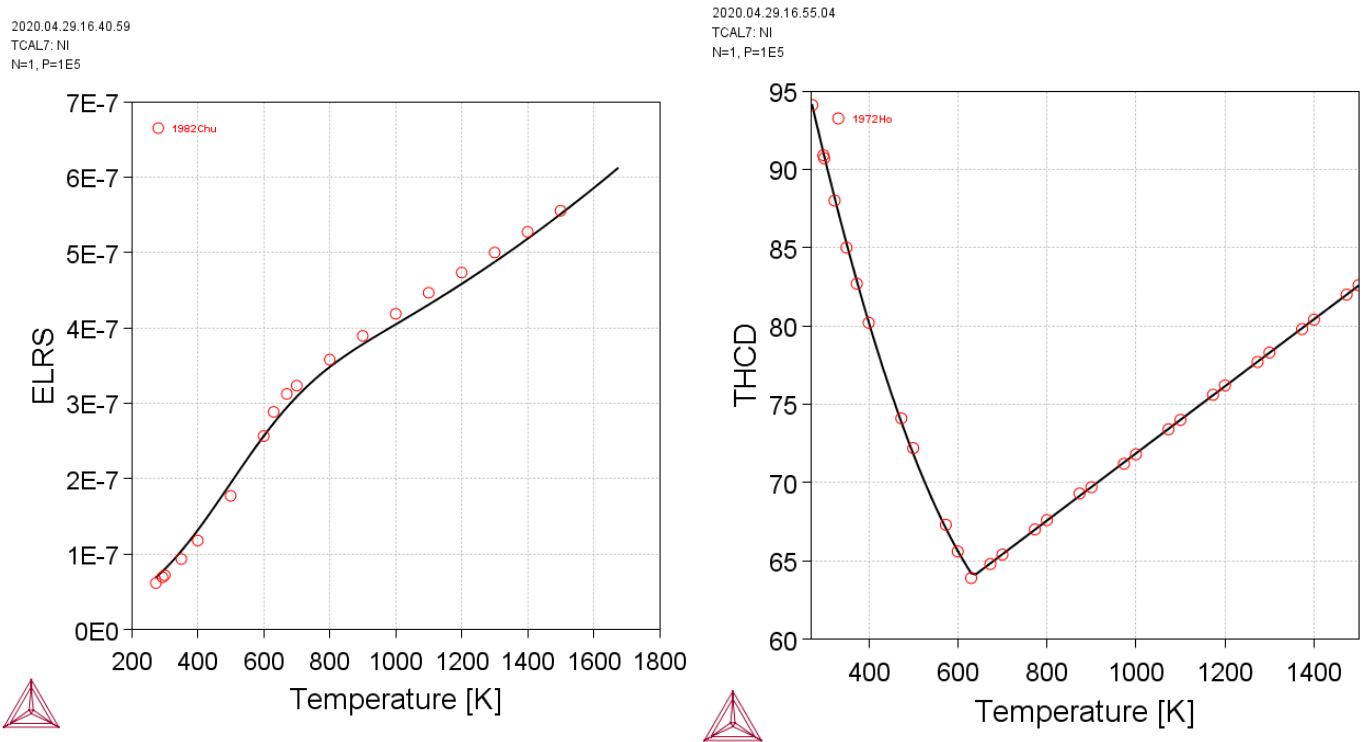


Figure 45: Modeling pure Ni electrical resistivity (left) and thermal conductivity (right).

[Figure 46](#) shows the contribution due to the spin-disordering scatterings (the red dotted line) and the phonon-electron scatterings (the green dotted line) to the electrical resistivity of an FCC_A1 Ni, in addition to the total electrical resistivity (the light green dotted-dashed line) and the experimental data from [1982Chu] (golden symbols in the plot). The residual resistivity is insignificant and included in the calculated total resistivity. As a user, you have access to the total resistivity via calculations with Thermo-Calc. This plot may help you understand how the modeling works.

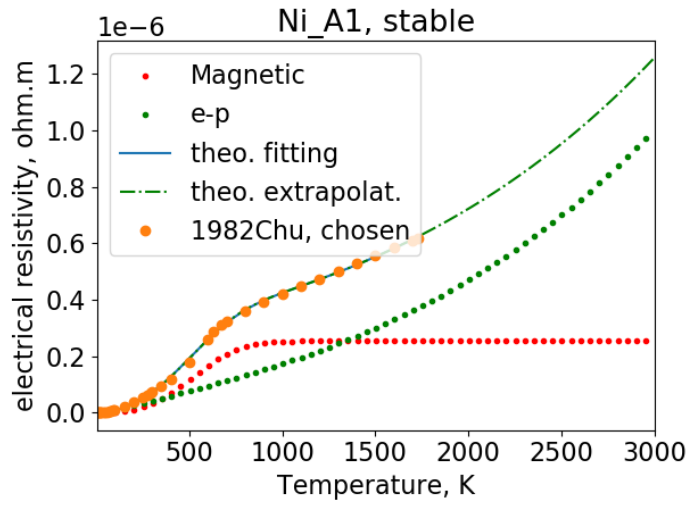


Figure 46: The modeling of electrical resistivity (ELRS) of FCC_A1 Ni compared to experimental data from [1982Chu]. See the text for details.

Cu: Thermal Conductivity

This example is of thermal conductivity for FCC_A1 Cu, which is an important alloying element to several series of aluminum alloys.



The extrapolation might not be valid beyond 3000 K.

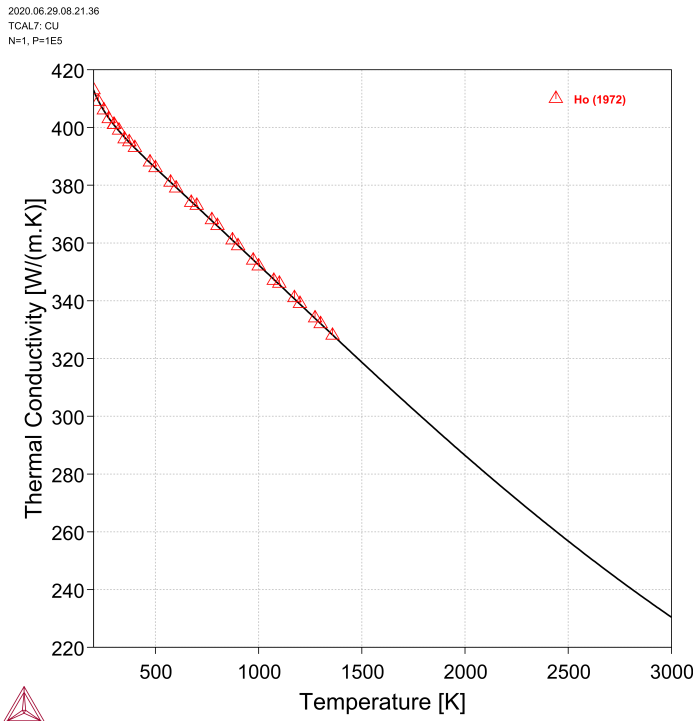


Figure 47: Calculated thermal conductivity (THCD) of FCC_A1 Cu compared to experimental data from [1972Ho].

Al-Mg: Electrical Resistivity

The example below shows calculated electrical resistivity of the Al-Mg FCC_A1 solid solution in a wide temperature range from 250 K to 850 K, in comparison with data recommended by Ho et al. [1983Ho], which were from “annealed” alloys. It should be noted that the calculations are performed with the global minimization setting turned off and with all the phases suspended except for FCC_A1. This is because the FCC_A1 single phase, which was obtained after being annealed and quenched, is assumed not to decompose or transform to another phase while it was exposed to the measuring temperatures for a short period of time. Based on the equilibrium Al-Mg phase diagram, it is suspected that certain alloys might contain ALMG_BETA depending on the metallurgy history and the alloy composition.

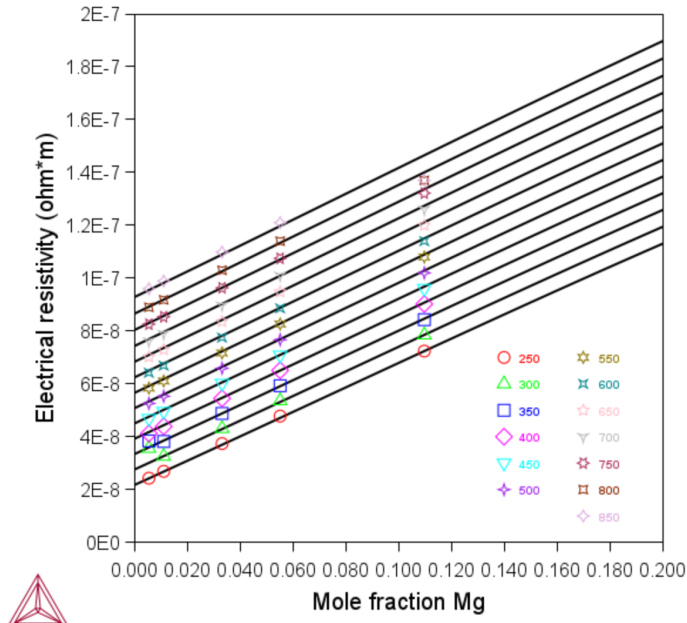


Figure 48: Electrical resistivity of Al-Mg single phase solid solution.

References

- [1972Ho] C. Y. Ho, R. W. Powell, P. E. Liley, Thermal Conductivity of the Elements, J.Phys. Chem. Reference Data 1, 279-421 (1972).
- [1982Chu] T. K. Chu, C. Y. Ho, Electrical resistivity of Chromium, Cobalt, Iron, and Nickel- CINDAS Report 60 (West Lafayette, Indiana, 1982).
- [1983Ho] C. Y. Ho, M. W. Ackerman, K. Y. Wu, T. N. Havill, R. H. Bogaard, R. A. Matula, S. G. Oh, H. M. James, Electrical Resistivity of Ten Selected Binary Alloy Systems, J. Phys. Chem. Reference Data 12, 183-322 (1983).

Viscosity: Al-Cu and Cu-Al-Si

The viscosity thermophysical property data is included with the TCS Al-based Alloy Database (TCAL) as of version 7 (TCAL7).

For more information about the various thermophysical, thermomechanical, and properties models, and when in Thermo-Calc, press F1 to search the online help. The details are found under a *General Reference* section.



You can find information on our website about the [properties that can be calculated](#) with Thermo-Calc and the Add-on Modules. Additional resources are added on a regular basis so keep checking back or [subscribe to our newsletter](#).

Al-Cu

Al-Cu and Al-Si are assessed based on experimental data. For Al-Cu, the data from Schick [2012Sch] is used for fitting the parameters but data from Konstantinova [2009Kon] is also shown.

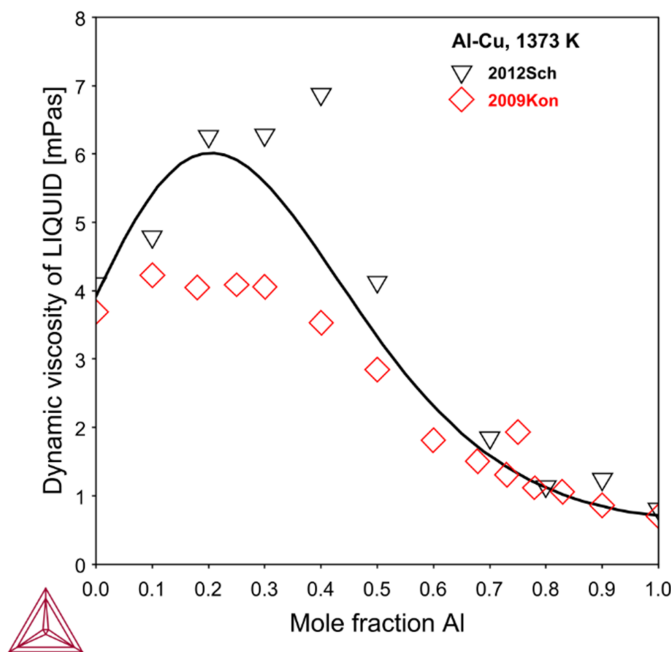


Figure 49: Calculated dynamic viscosity of Al-Cu at 1373 K along with experimental data from [2009Kon; 2012Sch].

Cu-Al-Si

The following plot shows the calculated viscosity of Cu-Al-Si alloys as a function of composition at 1375 K.

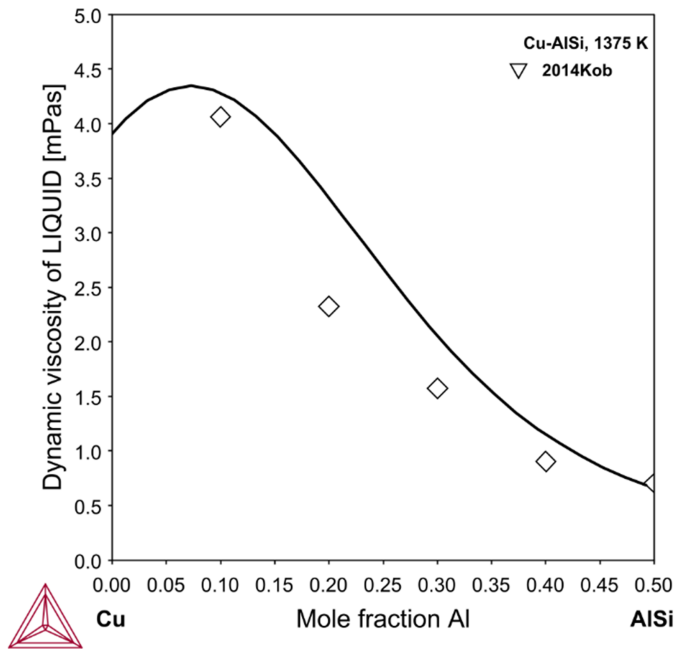


Figure 50: Calculated dynamic viscosity of Cu-Al-Si alloys at 1375 K is compared with the experimental data from [2014Kob].

References

- [2009Kon] N. Y. Konstantinova, P. S. Popel', D. A. Yagodin, The kinematic viscosity of liquid copper-aluminum alloys. *High Temp.* 47, 336–341 (2009).
- [2012Sch] M. Schick, J. Brillo, I. Egry, B. Hallstedt, Viscosity of Al–Cu liquid alloys: measurement and thermodynamic description. *J. Mater. Sci.* 47, 8145–8152 (2012).
- [2014Kob] H. Kobatake, J. Schmitz, J. Brillo, Density and viscosity of ternary Al–Cu–Si liquid alloys. *J. Mater. Sci.* 49, 3541–3549 (2014).

Surface Tension: Al-Cu and Ag-Al-Cu

The surface tension thermophysical property data is included with the TCS Al-based Alloy Database (TCAL) as of version 7 (TCAL7).

For more information about the various thermophysical, thermomechanical, and properties models, and when in Thermo-Calc, press F1 to search the online help. The details are found under a *General Reference* section.



You can find information on our website about the [properties that can be calculated](#) with Thermo-Calc and the Add-on Modules. Additional resources are added on a regular basis so keep checking back or [subscribe to our newsletter](#).

Al-Cu

The surface tension of Al-Cu liquid alloys at 1520 K is shown.

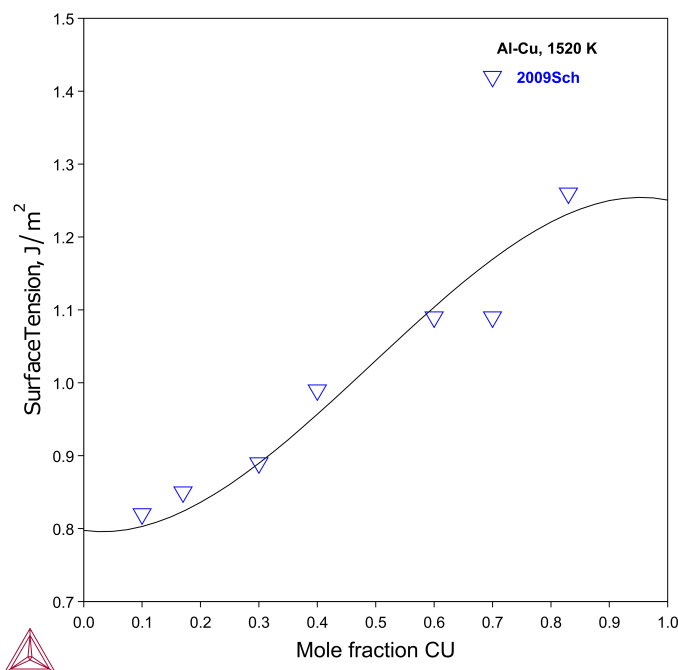


Figure 51: Calculated surface tension of Al-Cu at 1520 K along with experimental data from [2009Sch].

Ag-Al-Cu

The surface tension of Ag-Al-Cu liquid alloys are measured by Brillo [2014Bri] by electromagnetic levitation technique. Three isoplethal sections are shown.

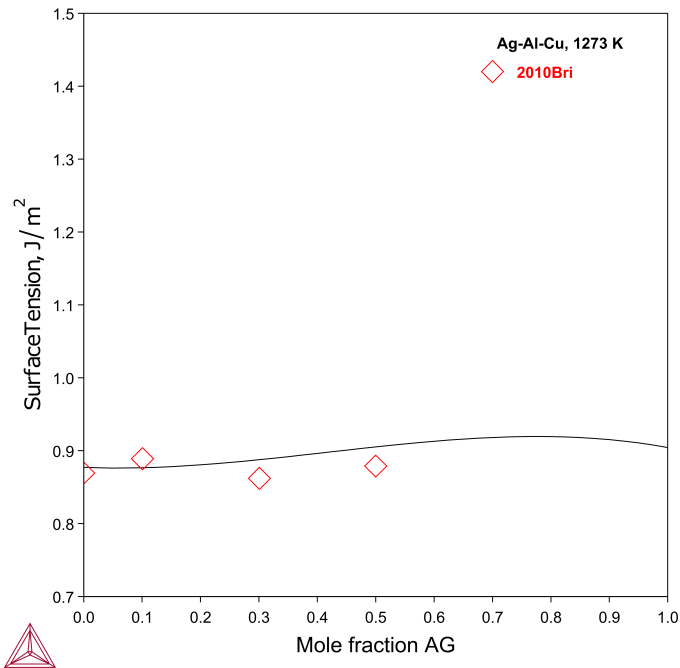


Figure 52: Calculated surface tension of an Ag-Al-Cu alloy at 1273 K along with experimental data from [2010Bri].

References

- [2009Sch] J. Schmitz, J. Brillo, I. Egry, R. Schmid-Fetzer, Surface tension of liquid Al–Cu binary alloys. *Int. J. Mater. Res.* 100, 1529–1535 (2009).
- [2010Bri] J. Brillo, Y. Plevachuk, I. Egry, Surface tension of liquid Al–Cu–Ag ternary alloys. *J. Mater. Sci.* 45, 5150–5157 (2010).
- [2010Fim] P. Fima, N. Sobczak, Thermophysical Properties of Ag and Ag–Cu Liquid Alloys at 1098K to 1573K. *Int. J. Thermophys.* 31, 1165–1174 (2010).
- [2014Bri] J. Brillo, G. Lauletta, L. Vaianella, E. Arato, D. Giuranno, R. Novakovic, E. Ricci, Surface Tension of Liquid Ag–Cu Binary Alloys. *ISIJ Int.* 54, 2115–2119 (2014).